

## 1 Preliminaries

**Definition 1.1.** Roots of the following quadratic equation are denoted as  $\beta$  and  $\beta'$ .

$$x^2 = 4x - 1 \quad \beta = 2 + \sqrt{3} \doteq 3.732 \quad \beta' = 2 - \sqrt{3} \doteq 0.268$$

*Remark 1.* The number  $\beta$  as defined in Definition 1.1 will represent the same value in the entire text.

Being roots of the same quadratic equation,  $\beta$  and  $\beta'$  have some interesting properties that are often used while working with quasicrystals.

**Theorem 1.2.** *Properties of the roots  $\beta$  and  $\beta'$ .*

$$\begin{aligned} \beta\beta' &= 1 & \beta^{k+2} &= 4 \cdot \beta^{k+1} - \beta^k & \frac{1}{\beta} &= \beta' = 4 - \beta \\ \beta + \beta' &= 4 & \beta'^{k+2} &= 4 \cdot \beta'^{k+1} - \beta'^k & \frac{1}{\beta'} &= \beta = 4 - \beta' \end{aligned}$$

**Definition 1.3.** Symbol  $\mathbb{Z}[\beta]$  denotes the smallest ring containing integers  $\mathbb{Z}$  and the irrationality  $\beta$ . Since  $\beta$  is quadratic the ring has the following simple form.

$$\mathbb{Z}[\beta] = \{a + b\beta \mid a, b \in \mathbb{Z}\}$$

*Remark 2.* Similarly, ring  $\mathbb{Z}[\beta']$  can be defined. According to the Theorem 1.2 the two rings are equivalent:  $\mathbb{Z}[\beta] = \mathbb{Z}[\beta']$ .

## 2 One-dimensional quasicrystals

To define a quasicrystal one more definition is needed. Function connecting a space of the quasicrystal with a space of the acceptance set called acceptance window.

**Definition 2.1.** Function  $\cdot' : \mathbb{Z}[\beta] \rightarrow \mathbb{Z}[\beta']$  is defined as  $(a + b\beta)' = a + b\beta'$ .

*Remark 3.* Notation is consistent with the Definition 1.1:  $(\beta)' = \beta'$ .

**Definition 2.2.** Let  $\Omega \subset \mathbb{R}$  be a bounded set with non-empty interior. Then **one-dimensional quasicrystal** with the window  $\Omega$  is denoted by  $\Sigma(\Omega)$  and defined as:

$$\Sigma(\Omega) = \{x \in \mathbb{Z}[\beta] \mid x' \in \Omega\}$$

*Remark 4.*  $\Sigma(\Omega)$  where  $\Omega \subset \mathbb{R}$  always denotes one-dimensional quasicrystal.

Some properties of one-dimensional quasicrystals are crucial for the algorithms used for the analysis.

**Theorem 2.3.** *Let  $\Omega, \tilde{\Omega} \subset \mathbb{R}$  and  $\lambda \in \mathbb{Z}[\beta]$ .*

$$\begin{aligned} \Omega \subset \tilde{\Omega} &\Rightarrow \Sigma(\Omega) \subset \Sigma(\tilde{\Omega}) & \Sigma(\Omega) \cap \Sigma(\tilde{\Omega}) &= \Sigma(\Omega \cap \tilde{\Omega}) \\ \Sigma(\Omega + \lambda') &= \Sigma(\Omega) + \lambda & \Sigma(\Omega) \cup \Sigma(\tilde{\Omega}) &= \Sigma(\Omega \cup \tilde{\Omega}) \\ \Sigma(\beta\Omega) &= \frac{1}{\beta}\Sigma(\Omega) \end{aligned}$$

*Remark 5.* Further only left-closed right-open intervals will be analyzed as windows. That is justified by theorem 2.3 and following analysis.

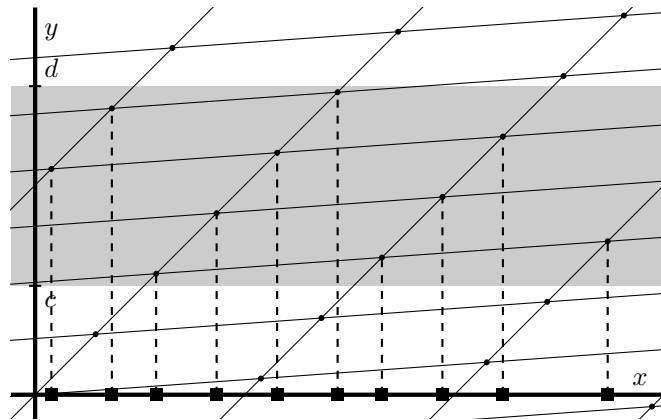


Figure 1: Illustration of one-dimensional quasicrystal. Grid intersections are defined as a set  $\{(\lambda, \lambda') | \lambda \in \mathbb{Z}[\beta]\}$ . There is a window  $\Omega = [c, d]$  on the  $y$  axis and finally the squares on the  $x$  axis are points of the quasicrystal  $\Sigma(\Omega)$ .

$$\begin{aligned}\Sigma((c, d)) &= \begin{cases} \Sigma([c, d]) & c \notin \mathbb{Z}[\beta] \\ \Sigma([c, d]) \setminus \{c'\} & c \in \mathbb{Z}[\beta] \end{cases} & \Sigma([c, d]) &= \begin{cases} \Sigma([c, d]) & d \notin \mathbb{Z}[\beta] \\ \Sigma([c, d]) \cup \{d'\} & d \in \mathbb{Z}[\beta] \end{cases} \\ \Sigma((c, d]) &= \begin{cases} \Sigma((c, d)) & d \notin \mathbb{Z}[\beta] \\ \Sigma((c, d)) \cup \{d'\} & d \in \mathbb{Z}[\beta] \end{cases}\end{aligned}$$

**Theorem 2.4.** Let  $\Omega \subset \mathbb{R}$  then  $\forall k \in \mathbb{Z} : \Sigma(\frac{1}{\beta^k} \Omega) = \beta^k \Sigma(\Omega)$ .

**Corollary 2.5.** From remark 5 and theorem 2.4 follows that only windows  $\Omega = [c, d]$  where  $d - c \in (\frac{1}{\beta}, 1]$  need to be analyzed. Such windows are called **base windows** or **windows in the base form**. Quasicrystals for all other windows can be acquired from the quasicrystals with the base windows by scaling and operations from remark 5.

## 2.1 One-dimensional quasicrystal structure

Figure 1 suggests that the one-dimensional quasicrystal is a sequence of points. This subsection presents an analysis of spacing and distribution of these points.

**Definition 2.6.** Strictly increasing sequence  $(y_n^\Omega)_{n \in \mathbb{Z}}$  defined as  $\{y_n^\Omega | n \in \mathbb{Z}\} = \Sigma(\Omega)$  where  $\Omega \subset \mathbb{R}$  is called the **sequence of quasicrystal**  $\Sigma(\Omega)$ .

**Theorem 2.7.** Let  $\Omega = [c, d]$  is a base window, then all possible distances between two immediately following points of the sequence of the quasicrystal  $\Sigma(\Omega)$ ,  $(y_{n+1}^\Omega - y_n^\Omega)$  are listed in the table 1.

*Remark 6.* Please notice that the cases for window sizes  $\frac{1}{\beta}$ ,  $\frac{\beta-2}{\beta}$ ,  $\frac{\beta-1}{\beta}$  and 1 each have only two different distances, therefore windows of these sizes are regarded as **singular**. Also distances for the size  $\frac{1}{\beta}$  are  $\beta$  multiples of the distances for the size 1.

**Definition 2.8.** The distances  $y_{n+1}^\Omega - y_n^\Omega$  are denoted:  $A = 4\beta - 1$ ,  $B = 3\beta - 1$ ,  $C = 2\beta - 1$ ,  $D = \beta$  and  $E = \beta - 1$ .

| $\frac{1}{\beta}$ | $\left(\frac{1}{\beta}, \frac{\beta-2}{\beta}\right)$ | $\frac{\beta-2}{\beta}$ | $\left(\frac{\beta-2}{\beta}, \frac{\beta-1}{\beta}\right)$ | $\frac{\beta-1}{\beta}$ | $\left(\frac{\beta-1}{\beta}, 1\right)$ | 1 |
|-------------------|---|-------------------------|---|-------------------------|---|---|
| $4\beta - 1$      | $4\beta - 1$  |                         |   |                         |   |   |
| $3\beta - 1$      | $3\beta - 1$  | $3\beta - 1$            | $3\beta - 1$  |                         |   |   |
| $\beta$           | $\beta$   | $\beta$                 | $\beta$   | $\beta$                 | $\beta$                                 |   |
|                   |   |                         | $2\beta - 1$  | $2\beta - 1$            | $2\beta - 1$                            |   |
|                   |   |                         |   | $\beta$                 | $\beta$                                 |   |
|                   |   |                         |   | $\beta - 1$             | $\beta - 1$                             |   |

Table 1: All possible distances between two immediately following points of the sequence of the quasicrystal with a window of the given size.

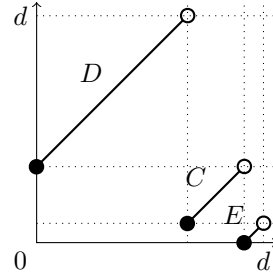


Figure 2: Graph of stepping function for quasicrystal  $\Sigma(\Omega)$  where  $\Omega = [c, d)$ ,  $c = 0$ ,  $d = 12 - 3\beta$ .  $C = 2\beta - 1$ ,  $D = \beta$  and  $E = \beta - 1$  (as in Definition 2.8).

**Definition 2.9.** Function  $f^\Omega : \Omega \rightarrow \Omega$  for  $\Omega = [c, d)$  defined as

$$d - c \in \left(\frac{1}{\beta}, \frac{\beta-2}{\beta}\right] : f^\Omega(x) = \begin{cases} x + (\beta)' & x \in [c, d - \frac{1}{\beta}) \\ x + (4\beta - 1)' & x \in [d - \frac{1}{\beta}, c + \frac{\beta-3}{\beta}) \\ x + (3\beta - 1)' & x \in [c + \frac{\beta-3}{\beta}, d) \end{cases}$$

$$d - c \in \left(\frac{\beta-2}{\beta}, \frac{\beta-1}{\beta}\right] : f^\Omega(x) = \begin{cases} x + (\beta)' & x \in [c, d - \frac{1}{\beta}) \\ x + (3\beta - 1)' & x \in [d - \frac{1}{\beta}, c + \frac{\beta-2}{\beta}) \\ x + (2\beta - 1)' & x \in [c + \frac{\beta-2}{\beta}, d) \end{cases}$$

$$d - c \in \left(\frac{\beta-1}{\beta}, 1\right] : f^\Omega(x) = \begin{cases} x + (\beta)' & x \in [c, d - \frac{1}{\beta}) \\ x + (2\beta - 1)' & x \in [d - \frac{1}{\beta}, c + \frac{\beta-1}{\beta}) \\ x + (\beta - 1)' & x \in [c + \frac{\beta-1}{\beta}, d) \end{cases}$$

is called the **stepping function** of the quasicrystal  $\Sigma(\Omega)$ .

*Remark 7.* Stepping function takes  $(\cdot)'$  image of a point of the quasicrystal and returns  $(\cdot)'$  image of immediately following point.

Stepping function is a valuable tool in theoretical quasicrystal analysis and has direct practical use in quasicrystal generation. Therefore the following theorem lists several key properties of this function.

**Theorem 2.10.** Let  $\Omega \subset \mathbb{R}$ :

- $f^\Omega((y_n^\Omega)') = (y_{n+1}^\Omega)'$   $\forall n \in \mathbb{N}$
- $(f^\Omega)^{-1}((y_{n+1}^\Omega)') = (y_n^\Omega)'$   $\forall n \in \mathbb{N}$
- $f^\Omega$  is piece-wise translation
- Discontinuities of  $f^\Omega$  divide the window  $\Omega$  into intervals. After the preimages of the points of one interval there is the same distance to the next point of the quasicrystal.

**Definition 2.11.** Discontinuities of the stepping function of the quasicrystal  $\Sigma(\Omega)$ , where  $\Omega = [c, d]$  in the base form, are denoted as  $a^\Omega$  and  $b^\Omega$ .

$$\begin{aligned} d - c \in \left( \frac{1}{\beta}, \frac{\beta-2}{\beta} \right] : & \quad a^\Omega = d - \frac{1}{\beta} \\ & b^\Omega = c + \frac{\beta-3}{\beta} \\ d - c \in \left( \frac{\beta-2}{\beta}, \frac{\beta-1}{\beta} \right] : & \quad a^\Omega = d - \frac{1}{\beta} \\ & b^\Omega = c + \frac{\beta-2}{\beta} \\ d - c \in \left( \frac{\beta-1}{\beta}, 1 \right] : & \quad a^\Omega = d - \frac{1}{\beta} \\ & b^\Omega = c + \frac{\beta-1}{\beta} \end{aligned}$$

*Remark 8.* Notation from previous definition will be often used to divide a base window  $\Omega = [c, d]$  into three disjunct intervals.

$$\Omega = [c, a^\Omega) \cup [a^\Omega, b^\Omega) \cup [b^\Omega, d)$$

For singular cases where  $d - c \in \left\{ \frac{\beta-2}{\beta}, \frac{\beta-1}{\beta}, 1 \right\}$ ,  $a^\Omega = b^\Omega$  and the window is then divided only in to two intervals  $[c, a^\Omega) \cup [a^\Omega, d)$ .

**Definition 2.12.** Let  $\Omega = [c, d]$ . The word  $(t_n^\Omega)_{n \in \mathbb{Z}}$  over the alphabet  $\{A, B, C, D, E\}$  is called the **word** of the quasicrystal  $\Sigma(\Omega)$ .

$$\begin{aligned} d - c \in \left( \frac{1}{\beta}, \frac{\beta-2}{\beta} \right] : \quad t_n^\Omega = & \begin{cases} D & y_{n+1}^\Omega - y_n^\Omega = \beta \\ A & y_{n+1}^\Omega - y_n^\Omega = 4\beta - 1 \\ B & y_{n+1}^\Omega - y_n^\Omega = 3\beta - 1 \end{cases} \\ d - c \in \left( \frac{\beta-2}{\beta}, \frac{\beta-1}{\beta} \right] : \quad t_n^\Omega = & \begin{cases} D & y_{n+1}^\Omega - y_n^\Omega = \beta \\ B & y_{n+1}^\Omega - y_n^\Omega = 3\beta - 1 \\ C & y_{n+1}^\Omega - y_n^\Omega = 2\beta - 1 \end{cases} \\ d - c \in \left( \frac{\beta-1}{\beta}, 1 \right] : \quad t_n^\Omega = & \begin{cases} D & y_{n+1}^\Omega - y_n^\Omega = \beta \\ C & y_{n+1}^\Omega - y_n^\Omega = 2\beta - 1 \\ E & y_{n+1}^\Omega - y_n^\Omega = \beta - 1 \end{cases} \end{aligned}$$

*Remark 9.* Word of the quasicrystal describes the distribution of the points of the quasicrystal.

**Definition 2.13.** Function  $\mathcal{C}_\ell : \mathbb{N} \rightarrow \mathbb{N}$ , that assigns to  $n \in \mathbb{N}$  number of different sub-words of the length  $n$  in the word of the quasicrystal  $(t_n^\Omega)_{n \in \mathbb{Z}}$  where  $|\Omega| = \ell$  is called the **complexity** of the quasicrystal.

**Definition 2.14.** Set  $\mathcal{L}_\ell(n)$  containing all different sub-words of the length  $n$  in the word of the quasicrystal  $(t_n^\Omega)_{n \in \mathbb{Z}}$  where  $|\Omega| = \ell$  is called the **language** of the quasicrystal.

*Remark 10.* Please note that the complexity and the language of the quasicrystal are defined dependent only on the length of the window.

That concludes the analysis of the one-dimensional quasicrystal for now. Additional findings will be presented later.

## Delone set and voronoi tessellation

Section provides the definitions of a delone set, a covering radius and a voronoi tessellation.

**Definition 2.15.** Let  $P \subset \mathbb{R}^n$  and  $\exists R > 0, \exists r > 0$ :

$$\forall x, y \in P, x \neq y : r \leq \|x - y\|$$

$$\forall z \in \mathbb{R}^n \exists x \in P : \|z - x\| \leq R$$

Then  $P$  is called **delone** set.

For each delone set  $P$  **covering radius** is defined as:

$$R_c = \inf\{R > 0 \mid z \in \mathbb{R}^n \exists x \in P : \|z - x\| \leq R\}$$

**Definition 2.16.** Let  $P \subset \mathbb{R}^n$ ,  $P$  is a discrete set and  $x \in P$ . Then

$$V(x) = \{y \in \mathbb{R}^n \mid \forall z \in P, z \neq x : \|y - x\| < \|y - z\|\}$$

is called **voronoi polygon** of  $x$  on  $P$ .

Voronoi polygon  $V(x)$  is said to belong to the point  $x$  and  $x$  is called the center of the polygon  $V(x)$ . The subset of  $P$  that directly shapes the polygon  $V(x)$  is called the domain of the polygon.

*Remark 11.* Example of a delone set with the voronoi tessellation can be seen in the Figure 5.

**Theorem 2.17.** Let  $P \subset \mathbb{R}^n$  is a delone set and  $R_c$  it's covering radius. For any  $x \in P$ :

$$N_x = \{z \in P \mid z \neq x \wedge \|z - x\| \leq 2R_c\}$$

Then voronoi tile of  $x$  on  $P$  is

$$V(x) = \bigcap_{z \in N_x} \{y \in \mathbb{R}^n \mid \|y - x\| < \|y - z\|\}$$

### 3 Two-dimensional quasicrystals

In the following section a two-dimensional quasicrystal is defined and analyzed. Thanks to the Theorem 3.4, analysis of one-dimensional quasicrystals can be in some way applied to the two-dimensional quasicrystals as well.

**Definition 3.1.** Vectors  $\alpha_1, \alpha_2, \alpha_3$  and the set  $M$  denote the following.

$$\alpha_1 = (1, 0) \quad \alpha_2 = \left( \frac{2-\beta}{2}, \frac{1}{2} \right) \quad \alpha_3 = \left( \frac{\beta-2}{2}, \frac{1}{2} \right)$$

$$M = \mathbb{Z}[\beta]\alpha_1 + \mathbb{Z}[\beta]\alpha_2$$

*Remark 12.* The vectors and the set from previous definition are key to two-dimensional quasicrystal definition. The set  $M$  is used as a two-dimensional equivalent to  $\mathbb{Z}[\beta]$  from the one-dimensional quasicrystal. Function from following definition is used as a two-dimensional equivalent to  $'$ .

**Definition 3.2.** Function  $* : M \rightarrow M$  is called **star** function:

$$v^* = (a\alpha_1 + b\alpha_2)^* = a'\alpha_1 + b'\alpha_3 \quad \forall a, b \in \mathbb{Z}[\beta]$$

*Remark 13.* Simple consequence of the Theorem 3.2 is that  $\alpha_1^* = \alpha_1$  and  $\alpha_2^* = \alpha_3$ .

**Definition 3.3.** Let  $\Omega \subset \mathbb{R}^2$  be bounded set with nonempty interior. Then **two-dimensional quasicrystal** with the window  $\Omega$  is defined as:

$$\Sigma(\Omega) = \{x \in M \mid x^* \in \Omega\}$$

*Remark 14.*  $\Sigma(\Omega)$  where  $\Omega \subset \mathbb{R}^2$  always denotes two-dimensional quasicrystal.

*Remark 15.* The same properties from the Theorem 2.3 for the one-dimensional quasicrystals apply to the two-dimensional quasicrystals as well.

To analyze the two-dimensional quasicrystals again only windows of a certain shape will be considered. That is sufficient because of the Remark 15. The chosen window shape is a rhombus.

**Theorem 3.4.** Let  $I = [c, d]$ , then for the rhombus  $\Omega = I\alpha_1^* + I\alpha_2^*$  and the quasicrystal  $\Sigma(\Omega)$ :

$$\Sigma(\Omega) = \Sigma(I)\alpha_1 + \Sigma(I)\alpha_2$$

*The size of the rhombus refers to the size of the interval  $|I|$  also a base rhombic window refers to a rhombic window constructed from a base window  $I$ .*

*Remark 16.* Note in the previous theorem that while  $\Omega \subset \mathbb{R}^2$  and so  $\Sigma(\Omega)$  is a two-dimensional quasicrystal,  $I \subset \mathbb{R}$  and so  $\Sigma(I)$  is a one-dimensional quasicrystal. Illustration of the construction is in the Figure 3. The same Theorem also applies to parallelogram shaped windows.

From the analysis of one-dimensional quasicrystals and the Theorem 3.4 follows that the two-dimensional quasicrystals are delone sets.

To analyze distribution of the points of a two-dimensional quasicrystal, voronoi tessellation is used. The goal is to catalog shapes of all voronoi tiles that appear in a quasicrystal with a rhombic window.

First an algorithm for generation of a finite section of a quasicrystal is presented.

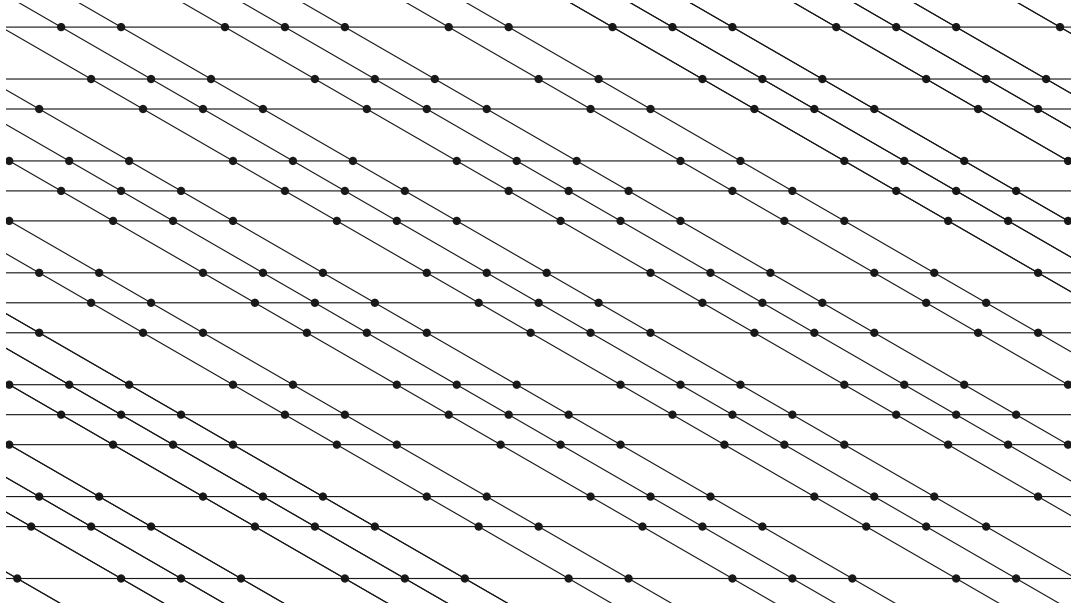


Figure 3: Illustration of the construction of the two-dimensional quasicrystal with a rhombic window from two one-dimensional quasicrystals. Horizontal lines mark copies of  $\Sigma(I)\alpha_1$  and the skewed lines mark copies of  $\Sigma(I)\alpha_2$ .

## 4 Generation of a finite section of a quasicrystal with a rhombic window

The algorithm is rather simple. It uses the stepping function and the Theorem 3.4.

**Algorithm definition** The algorithm receives as an input a rhombic window  $\Omega = I\alpha_1^* + I\alpha_2^*$  and bounds  $x_1, x_2, y_1, y_2 \in \mathbb{Z}[\beta]$ . The algorithm returns a subset of the quasicrystal  $\Sigma(\Omega)$  bounded by the given bounds.

$$\Sigma(\Omega) \cap ([x_1, x_2] \times [y_1, y_2])$$

First the one-dimensional interval  $I = [c, d)$  needs to be scaled and moved in such a way, that it becomes a base window and contains 0.

$$(\exists k \in \mathbb{Z})(\exists \lambda \in \mathbb{Z}[\beta]) : \left( I = \beta^k \tilde{I} + \lambda \right) \wedge \left( |\tilde{I}| \in \left( \frac{1}{\beta}, 1 \right] \right) \wedge \left( 0 \in \tilde{I} \right)$$

Now the stepping function can be used to iterate from 0 and generate enough points of the quasicrystal  $\Sigma(\tilde{I})$  to cover the bounds. However since the bounds are for the quasicrystal  $\Sigma(\Omega)$

they need to be transformed to be applicable to the quasicrystal  $\Sigma(\tilde{I})$ .

$$\begin{array}{ll} \tilde{x}_1 = x_1 & \tilde{y}_1 = 2y_1 \\ \tilde{x}_2 = x_2 + (\beta - 2)(y_2 - y_1) & \tilde{y}_2 = 2y_2 \end{array}$$

The stepping function is then used to acquire two sections of the quasicrystal  $\Sigma(\tilde{I})$ :  $\Sigma(\tilde{I}) \cap [\tilde{x}_1, \tilde{x}_2]$  and  $\Sigma(\tilde{I}) \cap [\tilde{y}_1, \tilde{y}_2]$ .

Each section needs to be transformed back:

$$\Sigma(I) = \beta^{-k}\Sigma(\tilde{I}) + \lambda'$$

and finally the finite section of the quasicrystal  $\Sigma(\Omega)$  is constructed:

$$\Sigma(\Omega) = \Sigma(I)\alpha_1 + \Sigma(I)\alpha_2$$

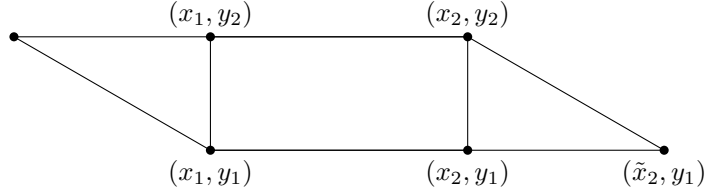


Figure 4: Illustration of how big parallelogram section of the quasicrystal (not a window) is needed to acquire a rectangular one.

*Remark 17.* Due to the way the two-dimensional quasicrystal is constructed, the result will contain more points than requested (Figure 4). However the excess points can be easily discarded.

The next goal is now to catalog all different voronoi polygons that appear in a quasicrystal for a single window.

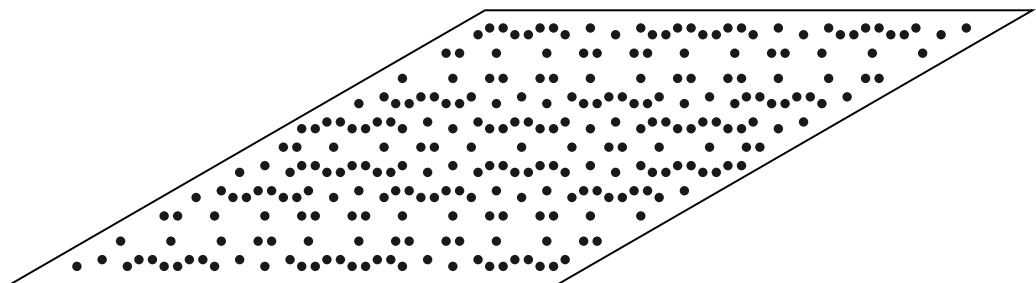
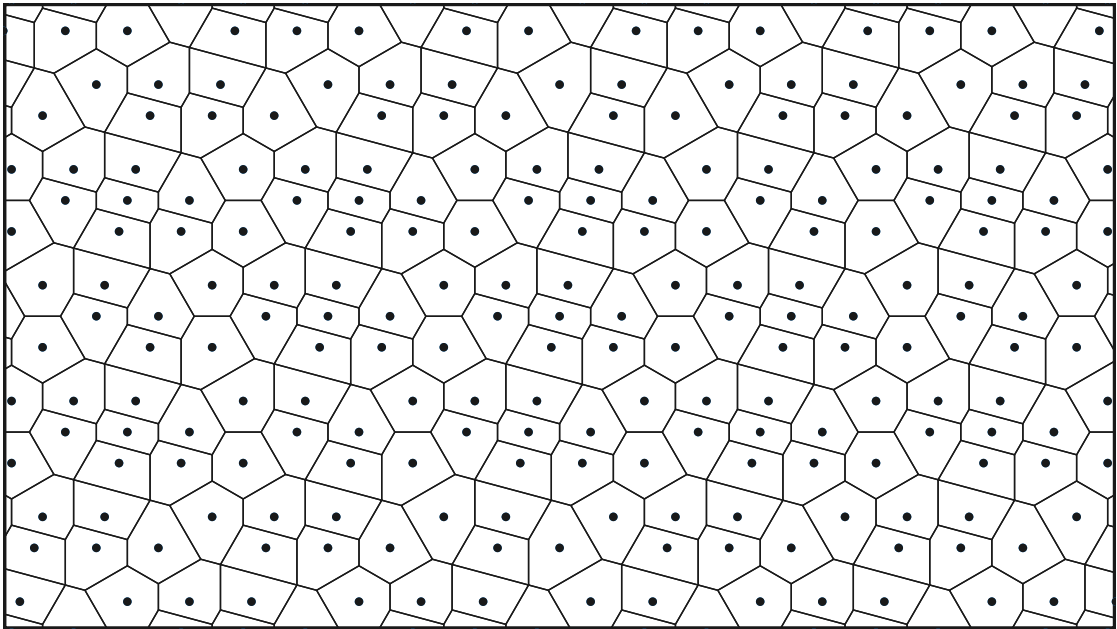


Figure 5: Finite section of the quasicrystal  $\Sigma(I\alpha_1^* + I\alpha_2^*)$  where  $|I| = \frac{6\beta-22}{7}$  with the voronoi tessellation and the rhombic window  $I\alpha_1^* + I\alpha_2^*$  with \* images of the points from the finite section.

## 5 Estimate of the covering radius

To catalog all different tiles that appear in a quasicrystal for a single window, all possible local configurations of the points of the quasicrystal need to be generated.

That is achieved by generating the language of the quasicrystal  $\mathcal{L}_n$  of a sufficient length that the finite sections corresponding to the words from the language  $\mathcal{L}_n$  cover the disk of the radius  $2R_c$  (in more detail in the next section), where  $R_c$  is the covering radius of the quasicrystal (Definition 2.15 and Theorem 2.17).

Since the precise value of  $R_c$  is difficult to evaluate, an upper bound estimate is used instead. As a reminder, here is the definition of the covering radius  $R_c$ , as is in Definition 2.15.

$$R_c = \inf\{R > 0 \mid z \in \mathbb{R}^n \exists x \in P : \|z - x\| \leq R\}$$

The estimate is derived from an artificial quasicrystal with only the largest distances between points (largest for the given window). Such quasicrystal has, for given window, certainly larger covering radius than any other. Since all such artificial quasicrystals are different only in scale and translation, the estimate is derived from a "normalized" one (a point in the origin and a unitized distance between points).

The estimate is then evaluated as the radius of a circumscribed circle or the circumradius  $R$  of a triangle with vertices  $(0, 0)$ ,  $(-1, 0)$  and  $\left(\frac{2-\beta}{2}, \frac{1}{2}\right)$ , as in Figure 6.

$$R_c \leq R = \frac{a}{2\sin(\alpha)} = \frac{1}{2 \left( \frac{1+\sqrt{3}}{2\sqrt{2}} \right)} = \frac{\sqrt{2}(\sqrt{3}-1)}{2}$$

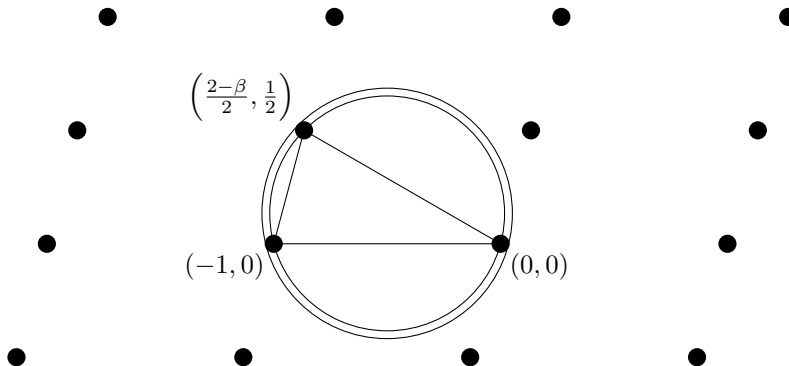


Figure 6: Section of the artificial quasicrystal with the circumcircle and a circle of the estimated radius  $\hat{R}_c$ .

Because the estimate is used in comparison with coordinates of the points of the quasicrystal, it is advantageous if it is also from  $\mathbb{Z}[\beta]$ . For that the estimate  $1.414 \doteq \sqrt{2} < 32\beta - 118 \doteq 1.426$  is used.

$$\frac{\sqrt{2}(\sqrt{3}-1)}{2} < \frac{(32\beta - 118)(\beta - 3)}{2} = 161 - 43\beta = \hat{R}_c \doteq 0.522$$

Since a unitized quasicrystal was used for the estimate, the value used in computation is the largest distance for a given window times  $\hat{R}_c$ .

*Remark 18.* There is an easier way that removes the need for such deriving. Simply estimate the covering radius with the largest distance itself. That is at first sufficient, but computational complexity of quasicrystals with a general window forced us to use all optimizations available.

## 6 Division of window

Previous section has established that for each point of the quasicrystal, the shape of the associated voronoi polygon is only influenced by the points of the quasicrystal that are closer than  $2L \cdot \hat{R}_c$ , where  $L$  is the largest distance for a given window.

In this section we describe the algorithm to divide one-dimensional window to parts by the same corresponding words. That is vital for two-dimensional quasicrystal analysis.

**Theorem 6.1.** *Function  $(f^\Omega)^n$  denotes the  $n$ -th iteration of the stepping function of the quasicrystal  $\Sigma(\Omega)$ . Set  $D_n = \{z_1 < z_2 < \dots < z_{m-1}\}$  contains all discontinuities of  $(f^\Omega)^n$ ,  $z_0 = c$  and  $z_m = d$ . Then  $(\forall i \in \hat{m} \cup \{0\})(\forall (y_l^\Omega)', (y_k^\Omega)' \in (z_i, z_{i+1}))$  are words  $t_l^\Omega t_{l+1}^\Omega \dots t_{l+n-1}^\Omega$  and  $t_k^\Omega t_{k+1}^\Omega \dots t_{k+n-1}^\Omega$  the same.*

*Remark 19.* In other words the Theorem 6.1 states that the discontinuities of the  $n$ -th iteration of the stepping function divide the window into intervals of images of the points of the quasicrystal after which the same sequence of distances of the length  $n$  follow.

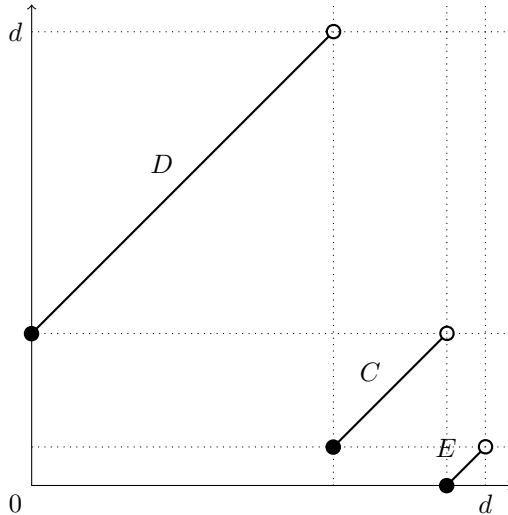


Figure 7: Graph of stepping function for quasicrystal  $\Sigma(\Omega)$  where  $\Omega = [c, d]$ ,  $c = 0$ ,  $d = 12 - 3\beta$ ,  $C = 2\beta - 1$ ,  $D = \beta$  and  $E = \beta - 1$ .

The algorithm uses the stepping function of a quasicrystal. As is apparent from Figure 7 and Theorem 2.10, stepping function is piece wise linear and after points of quasicrystal corresponding to one linear segment follows the same distance to the next point of the quasicrystal. Alternatively all the points of the sequence of the quasicrystal  $y_n$  whose images  $y'_n$  are in a single segment of linearity, have the same corresponding letter in the word of the quasicrystal. That is precisely what the algorithm uses.

First only non-singular windows are considered.

**Algorithm definition** Algorithm receives as an input an interval  $\Omega = [c, d]$  representing the window of the quasicrystal and  $n \in \mathbb{N}$  representing the desired length of the words.

As an output algorithm provides the division of  $\Omega$  into disjunct intervals  $[\omega_0, \omega_1), [\omega_1, \omega_2), \dots, [\omega_{m-1}, \omega_m)$  such that  $\omega_0 = c$  and  $\omega_m = d$ .

$$\left( \forall y_j^\Omega, y_k^\Omega \in (y_n^\Omega)_{n \in \mathbb{Z}} \right) \left( \forall i \in \widehat{m-1} \right) : \left( (y_j^\Omega)', (y_k^\Omega)' \in [\omega_i, \omega_{i+1}) \right) \Rightarrow \left( (t_n^\Omega)_j^{j+n} = (t_n^\Omega)_k^{k+n} \right)$$

The division is acquired by recursion.

For  $n = 1$  is the division already known.

$$m = 3, \omega_1 = a^\Omega, \omega_2 = b^\Omega$$

For  $n > 1$  is the division found from the division for  $n-1$ . Intervals  $[\omega_0^{n-1}, \omega_1^{n-1}), [\omega_1^{n-1}, \omega_2^{n-1}), \dots, [\omega_{m-1}^{n-1}, \omega_m^{n-1})$  denote the division for  $n-1$ .

For each interval  $[\omega_i^{n-1}, \omega_{i+1}^{n-1})$  the stepping function image is evaluated.

$$f^\Omega([\omega_i^{n-1}, \omega_{i+1}^{n-1})) = [f^\Omega(\omega_i^{n-1}), f^\Omega(\omega_{i+1}^{n-1}))$$

Then the image is divided by the points  $a^\Omega$  and  $b^\Omega$ . If one or both of these points are inside the image, it gets divided into two or three disjunct intervals.

After all intervals for  $i \in \widehat{k-1}$  are processed, all images or their divisions are sorted and denoted  $[\omega_0, \omega_1), [\omega_1, \omega_2), \dots, [\omega_{m-1}, \omega_m)$ .

For the singular windows  $a^\Omega = b^\Omega$  and so for  $n = 1$  the division becomes:

$$m = 2, \omega_1 = a^\Omega$$

At each step the image can be divided at most into two parts by the one point.

It may also be desirable to not only acquire the division of the window by the same words, but to also acquire the words themselves. That is done by a simple modification of the described algorithm. Each interval is marked with the corresponding letter  $A, B, C, D$  or  $E$  at the beginning of the recursion. While dividing the image of the interval by the points  $a^\Omega$  and/or  $b^\Omega$ , the mark is appended by an appropriate letter.

**Summary** For given  $n \in \mathbb{N}$  and window  $I = [c, d)$  is the language  $\mathcal{L}_{d-c}(n)$  finite and the described algorithm provides every word from the language. The next section takes together finite section generation, covering radius estimate and the language  $\mathcal{L}_\ell(n)$  to provide catalog of all shapes of voronoi polygons for a given window.

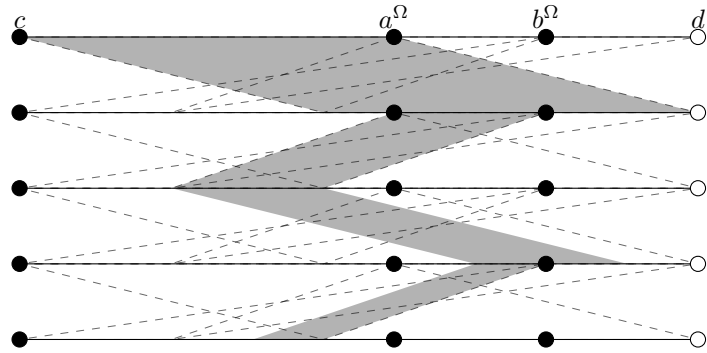


Figure 8: Iteration of the stepping function  $f^\Omega$  where  $|\Omega| = \frac{3\beta-10}{2}$ . Dashed lines show the exchange of intervals of the stepping function and the gray area shows progression of division for one interval.

## 7 Cataloging voronoi polygons for a single rhombic window

This section describes the algorithm for generating all voronoi polygons in a quasicrystal with a rhombic window. Unless otherwise stated, in this section quasicrystal always means two-dimensional quasicrystal and window always means rhombic window. The key components from previous sections are:

1. only the points of the quasicrystal that are close enough determine the shape of the voronoi polygon
2. finite section of the quasicrystal is easy to generate from two one-dimensional quasicrystals
3. language  $\mathcal{L}_\ell(n)$  is finite and easy to generate

There is a correspondence between a section of a word of a one-dimensional quasicrystal and a finite section of the one-dimensional quasicrystal.

$$t_m t_{m+1} \dots t_{m+k-1} t_{m+k} \longleftrightarrow y_m, y_{m+1}, \dots, y_{m+k-1}, y_{m+k}, y_{m+k+1}$$

$$y_{i+1} - y_i = t_i$$

Where the last equality is in terms of the Definition 2.8.

The algorithm is then straight forward:

**Algorithm definition** The algorithm receives as an input a rhombic window. As an output it returns a list of voronoi polygons found in the quasicrystal corresponding to the given window.

The largest distance within the corresponding one-dimensional quasicrystal is denoted by  $L$ .

1. evaluate  $L \cdot \hat{R}_c$  estimate of the covering radius of the quasicrystal
  2. determine the length of a word  $n$  sufficient to cover a circle of radius  $2L \cdot \hat{R}_c$  (described in more detail below)
  3. generate the language  $\mathcal{L}_\ell(n)$
- |          |          |          |
|----------|----------|----------|
| BBDBDBBD | DBBDBDBD | BDBDBBDB |
| DBDBDBBD | DBBDBDBB | BDBBDBDB |
| DBDBBDBD | BDBDBDBB | BBDBDBDB |
4. generate finite sections of the quasicrystal for each pair of the words from the language  $\mathcal{L}_\ell(n)$  such that each finite section contains origin (Figure 9)
  5. construct a voronoi polygon for the origin for each finite section (Figure 10)

To justify that the algorithm finds all voronoi polygons for a given window consider, that the shape of each voronoi polygon is determined by the points of the quasicrystal, that are distant at most  $2L \cdot \hat{R}_c$  from the center of the polygon. In other words, the shape is only determined by a finite section of the quasicrystal. Each finite section of the quasicrystal with a rhombic window is described by two finite sections of a one-dimensional quasicrystal. Each finite section of one-dimensional quasicrystal with  $n+1$  points is described by a finite word of the quasicrystal, every such word is present in the language  $\mathcal{L}_\ell(n)$ .

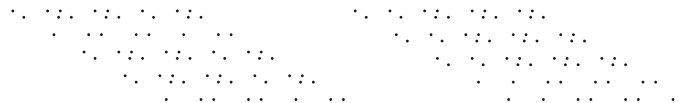


Figure 9: Example of just 2 finite sections.

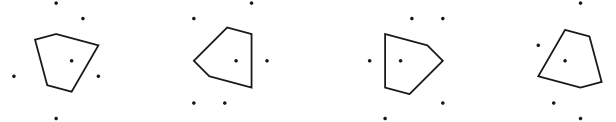


Figure 10: Example of one voronoi polygon in four different orientations.

### 7.1 Determine sufficient $n$

Part of the algorithm that was not covered in detail is how to determine the length of a word sufficient to cover a circle of radius  $2L \cdot \hat{R}_c$ . First a rhombus is circumscribed to the circle of the radius  $2L \cdot \hat{R}_c$ . The side of such rhombus is 4 times larger than the circle radius. Then such  $n$  has to be found that a finite section of one-dimensional quasicrystal corresponding to each word from  $2L \cdot \hat{R}_c$  has to be at least as long as the side of the circumscribed rhombus. There are several approaches, two are described here.

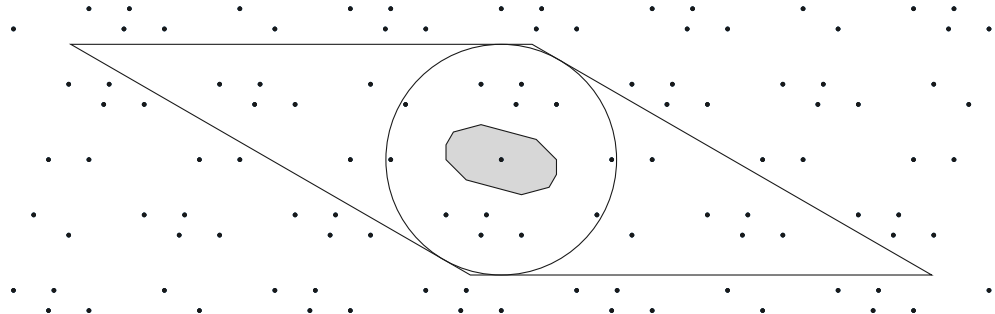


Figure 11: Finite section of a quasicrystal containing the origin. The circle has a radius  $2L \cdot \hat{R}_c$  and contains all the points of the quasicrystal that determine the shape of the voronoi polygon for the origin. The circumscribed rhombus contains a superset.

One way is to get the smallest distance  $S$  for the one-dimensional quasicrystal and set  $n = \left\lceil \frac{8L \cdot \hat{R}_c}{S} \right\rceil$ .

The second way is to start with  $n = 2$ , test each word of the language and increase by 1 until  $n$  sufficient.

The second way takes more time to compute but produces better estimate, which will be desirable once analyzing quasicrystals with a general window.

## 7.2 Different orientations

As is apparent from the figure 10, the same shape of a voronoi polygon appears in the quasicrystal in more orientations. This subsection covers analysis of different orientations of voronoi polygons.

It is helpful to see the connection between the domain of the voronoi polygon and it's \* image in the window of the quasicrystal. Figure 12 shows a voronoi polygon from the quasicrystal with the window size  $2 - 7\beta$ , the window and \* image of it's domain and it's center.

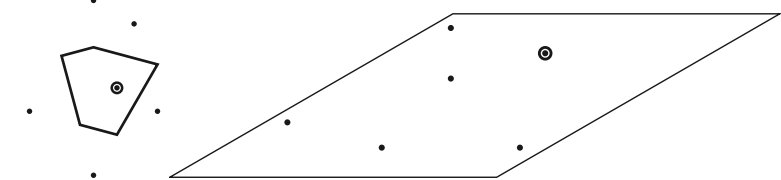


Figure 12: A voronoi polygon with it's center and domain and the \* image in the window of the quasicrystal.

It is clear that a voronoi polygon can appear in a quasicrystal only if the \* image of it's domain and center fits inside the window. Therefore a section of the window can be associated with a voronoi polygon through it's center. The section shows where in the window the \* image of the center can be so that the \* image of the domain fits in also (Figure 13).

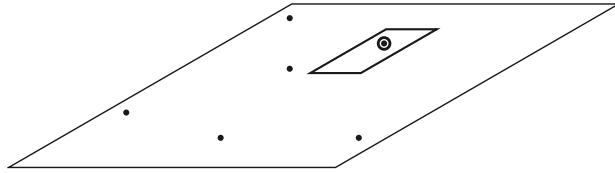


Figure 13: A window with the \* image of the domain and the center from the Figure 12 with the associated section.

In fact the entire window can be divided in such sections. Every point of the quasicrystal whose \* image falls within one section is the center of a voronoi polygon of the same shape (Figure 14). The algorithm for producing such division will be covered in the next section.

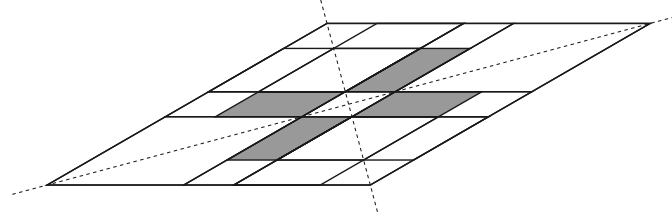


Figure 14: A window with the division into sections by the shape of corresponding voronoi polygon.

From the division two axis of symmetry are apparent. These are the sources of the different orientations of the voronoi polygons of the same shape. The highlighted sections in the Figure 14 correspond to the four voronoi polygons form the Figure 10

### 7.3 Dividing a rhombic window into sections by the shape of the corresponding voronoi polygon

Algorithm for checking whether a set of points belong to the quasicrystal also produces the shape of the section of the window.

Let  $\Omega$  be a rhombic window,  $V$  one of the voronoi polygons in the quasicrystal  $\Sigma(\Omega)$ ,  $c \in M$  the center of  $V$ ,  $D = \{p_1, \dots, p_k \in M\}$  the domain of  $V$  and  $q_i = p_i - c$ ,  $i \in \hat{k}$ . Then the  $*$  image of the center and the domain fit inside the window:

$$c^* \in \Omega \quad \wedge \quad c^* + q_i^* \in \Omega \quad (\forall i \in \hat{k})$$

which is equivalent to checking whether the image of the center  $c^*$  fits inside translated windows:

$$c^* \in \Omega \quad \wedge \quad c^* \in \Omega - q_i^* \quad (\forall i \in \hat{k})$$

$$c^* \in \left( \bigcap_{i \in \hat{k}} (\Omega - q_i^*) \right) \cap \Omega$$

Now first if the intersection is not empty then the polygon  $V$  appears in the quasicrystal  $\Sigma(\Omega)$ , this finding will be useful while analyzing quasicrystals with a general window. Also the intersection shows exactly the desired section of the window. Only if the image of the center fits inside this intersection does the image of the domain fit inside the window and that determines the shape of the voronoi polygon.

There is however a slight caveat. The intersection might be larger than the desired section. Consider this example, in the so far analyzed quasicrystal with the window size  $2\beta - 7$  there is a tile very similar in shape to the one in the Figure 10 (Figure 15).

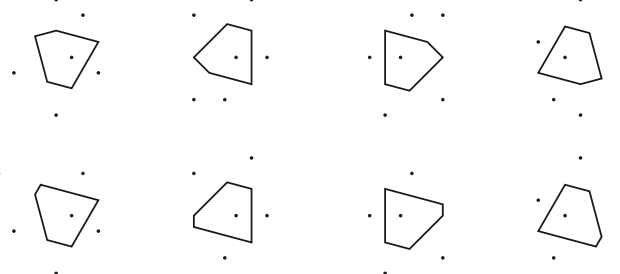


Figure 15: First line are the polygons from the Figure 10 and the second line are the slightly larger ones that also appear in the quasicrystal.

Therefore the intersection is a superset of the section. The Figure 16 shows the intersections for first polygons of each line in the Figure 15.

Clearly the first intersection is a subset of the second one and also the corresponding polygons are in the same relation. Therefore a conclusion can be drawn that if the  $*$  image falls within the smaller intersection, it's polygon will be the smaller one because the domain of the smaller polygon will be present in the quasicrystal. Only if the  $*$  image of the center fall outside the smaller intersection but inside the larger one will it's polygon be the larger one (Figure 17).

Similar situation happens with the polygons in the Figure 18.

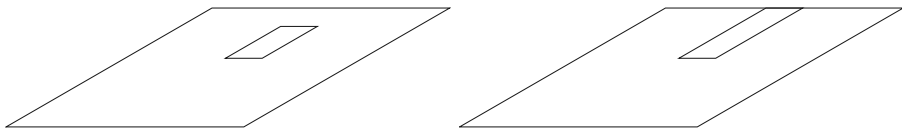


Figure 16: Intersections for first polygons in each line in the Figure 15.

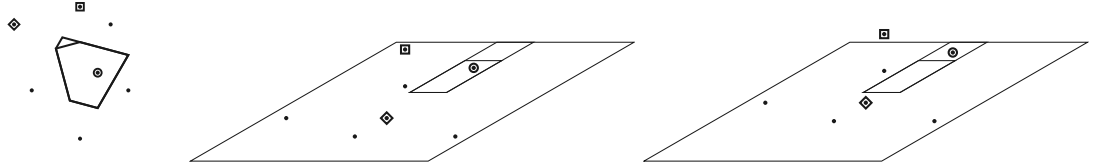


Figure 17: The points in the left window correspond to the smaller polygon, the  $\diamond$  marked point is not a member of the domain. The points in the right window correspond to the larger polygon, the  $\square$  marked point no longer fit inside the window and so the  $\diamond$  marked point becomes a member of the domain.

**Summary** This section covered the algorithms for generating all different shapes of voronoi polygons for a single rhobic window and for dividing said window into sections by the different shapes. Next section will achieve the same for all rhombic window sizes.

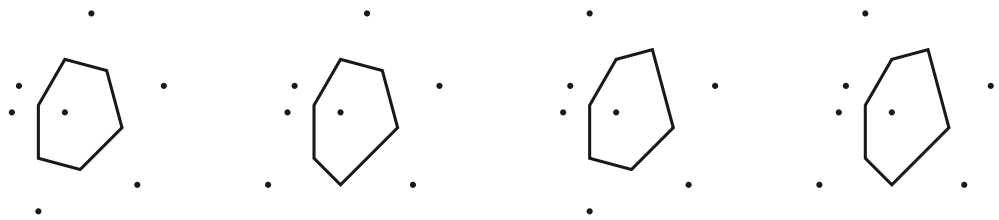


Figure 18: These voronoi polygons also have overlapping intersections.

## 8 Cataloging voronoi polygons for all rhombic windows

To catalog all different shapes of voronoi polygons in all quasicrystals with a rhombic window, several simplifications are put in place. First only base rhombic windows are considered since polygons from other quasicrystals are not different in shape only in scale. Secondly the base windows are divided by the same language in finitely many groups.

**Theorem 8.1.** Let  $\Omega = [c, c + \ell]$ .

If  $\ell \notin \mathbb{Z}[\beta]$  then  $\mathcal{C}_\ell(n) = 2n + 1$ ,  $\forall n \in \mathbb{N}$ .

If  $\ell \in \mathbb{Z}[\beta]$  then  $\exists^1 k \in \mathbb{N}$  such that  $((f^\Omega)^k(a^\Omega)) = b^\Omega$  or  $((f^\Omega)^{k+1}(b^\Omega)) = a^\Omega$  and

$$\mathcal{C}_\ell(n) = \begin{cases} 2n + 1 & \forall n \leq k \\ n + k + 1 & \forall n > k \end{cases}$$

**Theorem 8.2.** Let  $\Omega = [c, c + \ell]$ .

$$\mathcal{D}_n = \left\{ \ell \mid \ell \in \left( \frac{1}{\beta}, 1 \right] \wedge \mathcal{C}_\ell(n) < 2n + 1 \right\}$$

Then elements of  $\mathcal{D}_n$  divide interval  $I := \left( \frac{1}{\beta}, 1 \right]$  into finite amount of disjoint sub-intervals  $(I_m)_{m \in \hat{\mathbb{N}}}$  such that  $\mathcal{L}_{\ell_1}(n) = \mathcal{L}_{\ell_2}(n)$   $\forall \ell_1, \ell_2 \in I_m, \forall m \in \hat{\mathbb{N}}, \forall n \in \mathbb{N}$ .

*Remark 20.* Please note that  $\mathcal{D}_n$  from theorem 8.2 divides base windows into sets by the same language whereas  $D_n$  from theorem 6.1 divides specific window into intervals by the sequences of points that follow.

Previous two theorem give a guide to which points divide the base windows into groups of the same language and also how to find those points.

Now is the time to introduce new view on the one-dimensional base windows as a whole. Figure 19 shows a plot of all base windows side by side.

It shows well how the window changes while increasing in size and how the singular windows come to existence. However more importantly it shows that  $\mathcal{D}_1 = \left\{ \frac{\beta-2}{\beta}, \frac{\beta-1}{\beta} \right\}$ . The algorithm for generating  $\mathcal{D}_n$  is very similar to the algorithm for division of a single window or the algorithm for generating  $D_n$ . Only this time instead of getting a stepping function image of the endpoints of interval, the function is used on whole line segments representing  $a^\Omega$  and  $b^\Omega$ . Every time images of these line segments intersect a new point is added to the set  $\mathcal{D}_n$ .

For a sufficient  $n$ , such  $\mathcal{D}_n$  can be constructed that the same language on the subintervals implies the same set of different shapes of voronoi polygons on corresponding quasicrystals. The endpoints of the subintervals are then examined independently.

Such  $n$  is determined by the algorithm from the previous section. For the base windows there are three combinations of the largest and smallest distance possible:  $A, D$ ;  $B, D$  and  $C, E$ . The  $n$  is determined for each and the largest is selected. The first approach is used.

$$n_1 = \left\lceil \frac{8A \cdot \hat{R}_c}{D} \right\rceil = 16 \quad n_2 = \left\lceil \frac{8B \cdot \hat{R}_c}{D} \right\rceil = 12 \quad n_3 = \left\lceil \frac{8C \cdot \hat{R}_c}{E} \right\rceil = 10$$

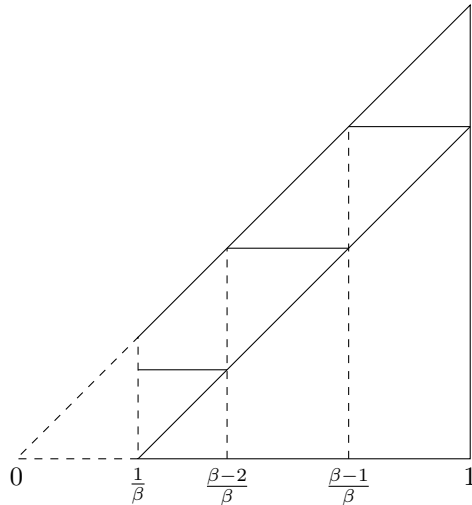


Figure 19: One-dimensional base windows. Each vertical slice represents one base window. The skewed line marks the point  $a^\Omega$  and the horizontal lines mark the point  $b^\Omega$ .

Therefore  $n = 16$  and  $\mathcal{D}_{16}$  is constructed. To generate all possible voronoi polygons in all quasicrystals with base windows, the algorithm from the previous section is used on all rhombic windows with a side  $\ell \in \mathcal{D}_{16}$  and for any  $\ell \in I_m$  for each of the disjoint intervals. Thus the voronoi polygons will be analyzed for each different language  $\mathcal{L}_\ell(16)$ , which is sufficient for analysis of every different voronoi polygon.

However the resulting set of voronoi polygons from  $\mathcal{D}_{16}$  is identical to the set of voronoi polygons for  $\mathcal{D}_4$  and is different from the one for  $\mathcal{D}_3$ . Thus it is assumed, that the generous estimates inflated the  $n$  greatly and  $n = 4$  is sufficient.

**Summary** This section covered the method for generating a catalog of all different voronoi polygons for all quasicrystals with base windows. Additionally it finalized the sufficient  $n$  as  $n = 4$ .

The next section will conclude the analysis of the two-dimensional quasicrystal with rhombic windows with the catalog of all different voronoi polygons.

## 9 Catalog of voronoi polygons for a rhombic window

As concluded in the previous section the sufficient  $n = 4$ .

$$\mathcal{D}_4 = \{4 - \beta, 10\beta - 37, 19 - 5\beta, 6\beta - 22, 2\beta - 7, 8 - 2\beta, 5\beta - 18, \beta - 3, 12 - 3\beta, 4\beta - 14, 1\}$$

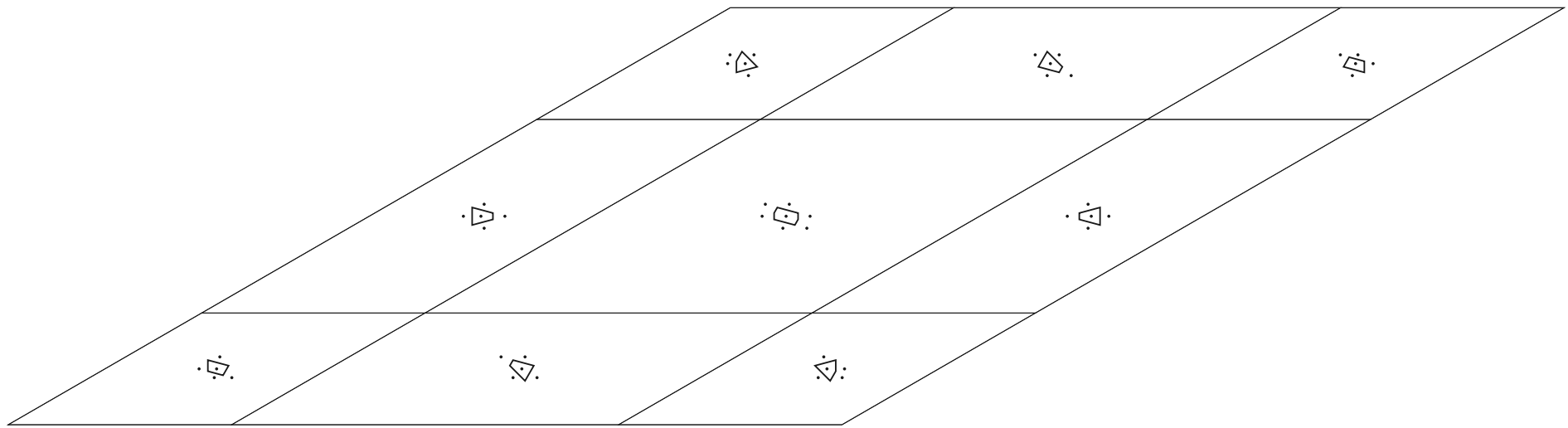
The endpoints  $4 - \beta$  and 1 are added for ease of use. To get the full set of sizes of rhombic windows that need to be analyzed a mean of each two consecutive numbers from  $\mathcal{D}_4$  is added. These represent the intervals of the same language.

$$\begin{aligned} \mathcal{D} = \left\{ 4 - \beta, \frac{9\beta - 33}{2}, 10\beta - 37, \frac{5\beta - 18}{2}, 19 - 5\beta, \frac{\beta - 3}{2}, 6\beta - 22, \right. \\ \left. \frac{8\beta - 29}{2}, 2\beta - 7, \frac{1}{2}, 8 - 2\beta, \frac{3\beta - 10}{2}, 5\beta - 18, \frac{6\beta - 21}{2}, \beta - 3, \right. \\ \left. \frac{9 - 2\beta}{2}, 12 - 3\beta, \frac{\beta - 2}{2}, 4\beta - 14, \frac{4\beta - 13}{2}, 1 \right\} \end{aligned}$$

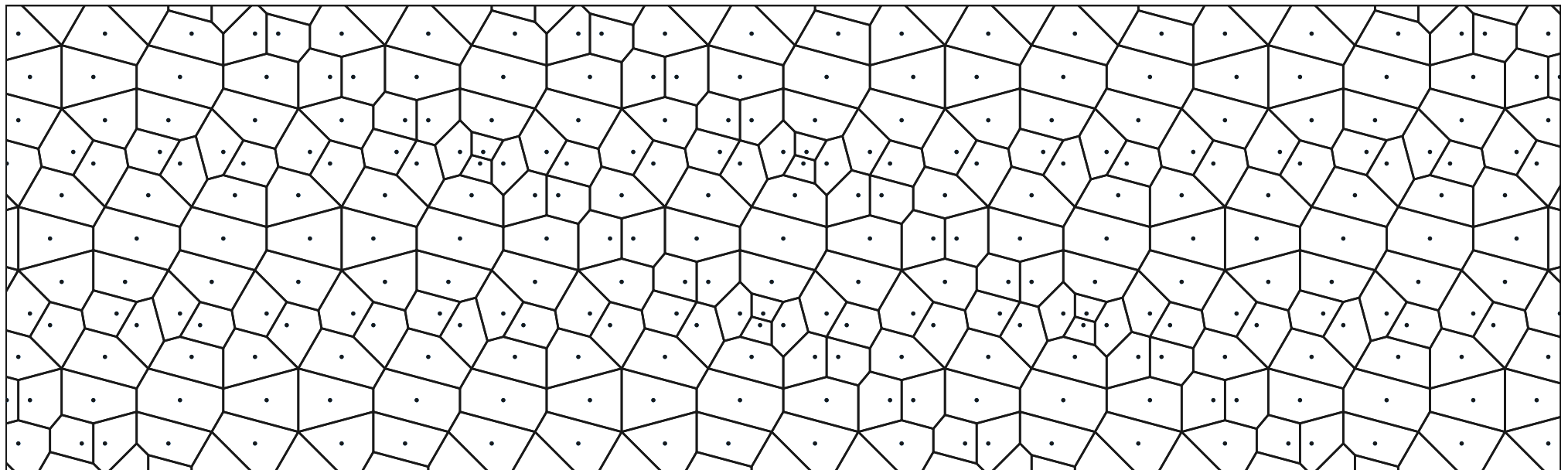
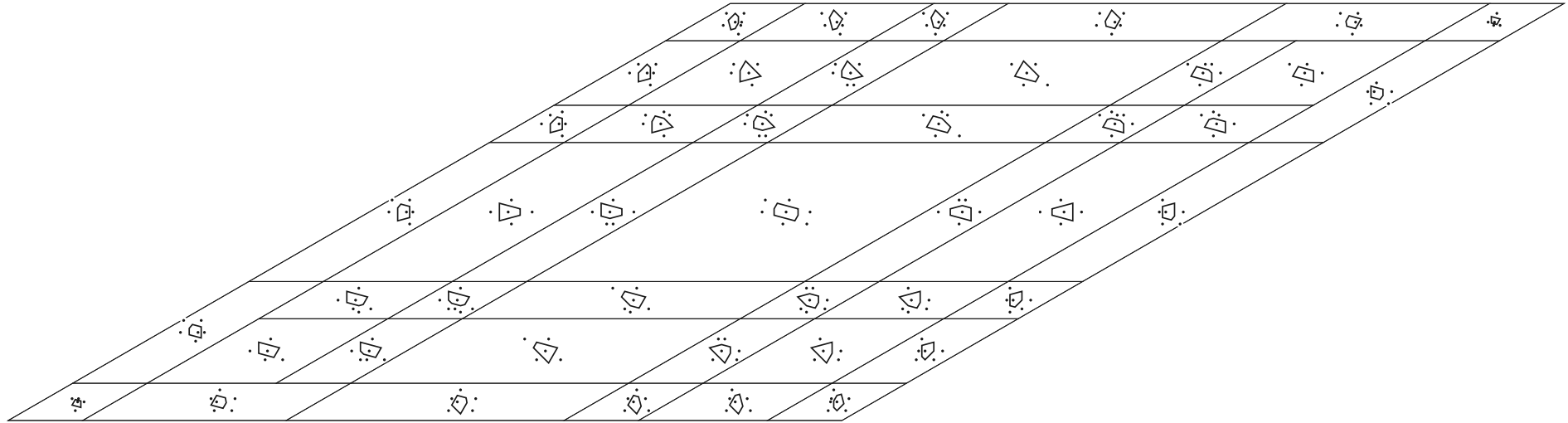
Following is a list of windows for each size in  $\mathcal{D}$  divided in sections by the corresponding voronoi polygon accompanied by a finite section of corresponding quasicrystal. The window for 1 looks identical as the window for  $4 - \beta$  because  $\beta\Sigma(\Omega^1) = \Sigma(\Omega^{4-\beta})$ .

The windows have been scaled to fit the page therefore the size of the polygons seem to decrease with growing window size. The finite sections of the quasicrystals do have the same scale.

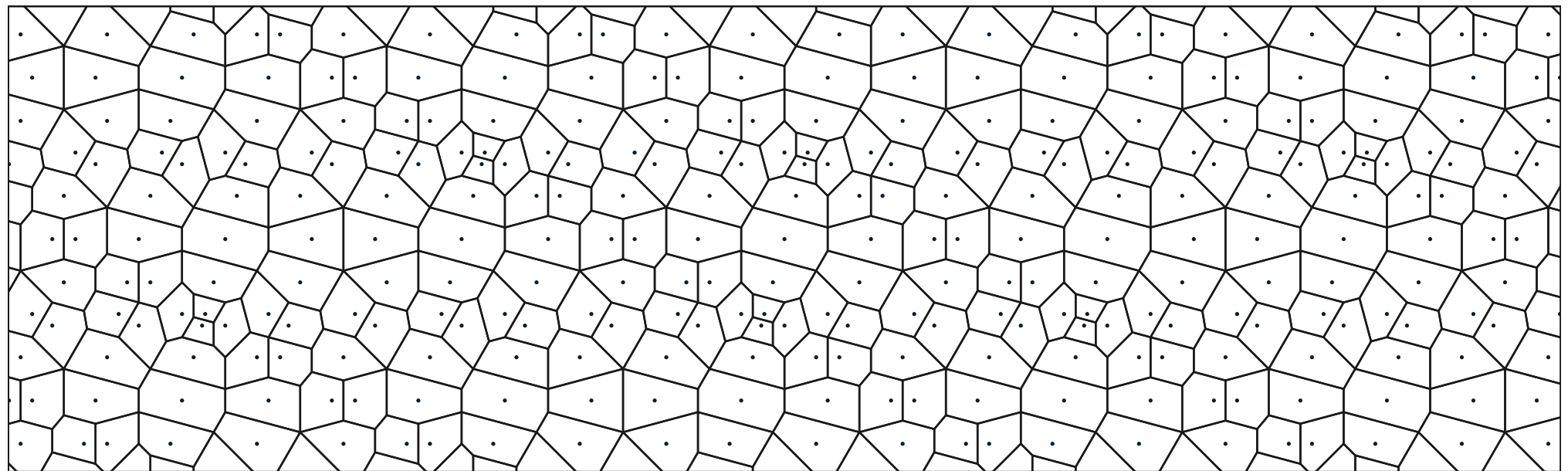
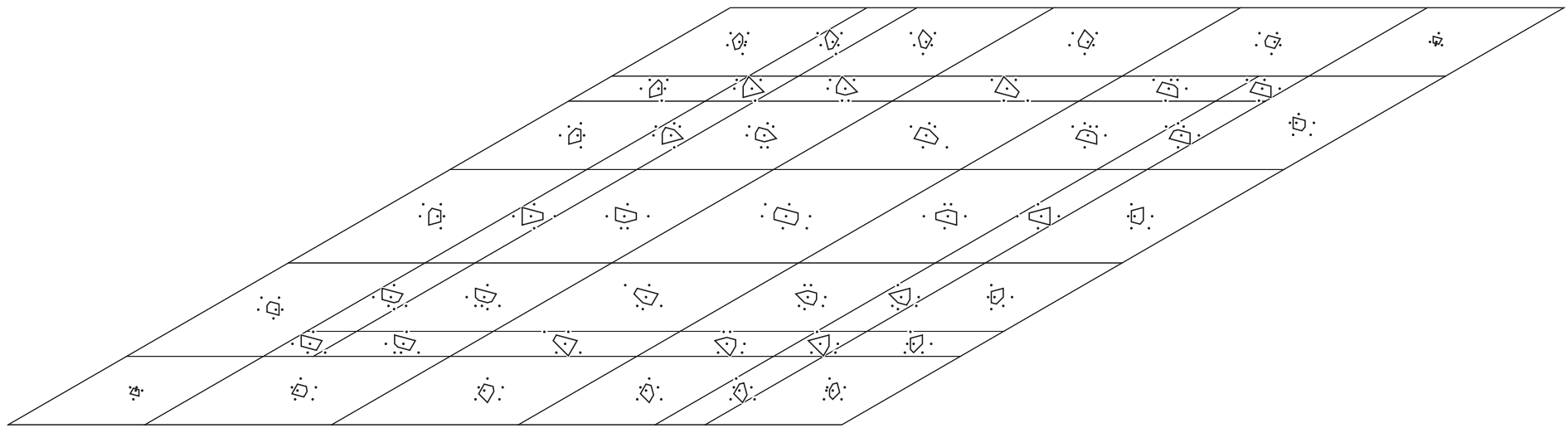
The catalog is then concluded by a list of all voronoi polygons for quasicrystals with base windows and a table assigning the polygons to the quasicrystals. In the list for each polygon only one orientation is selected if more are available.

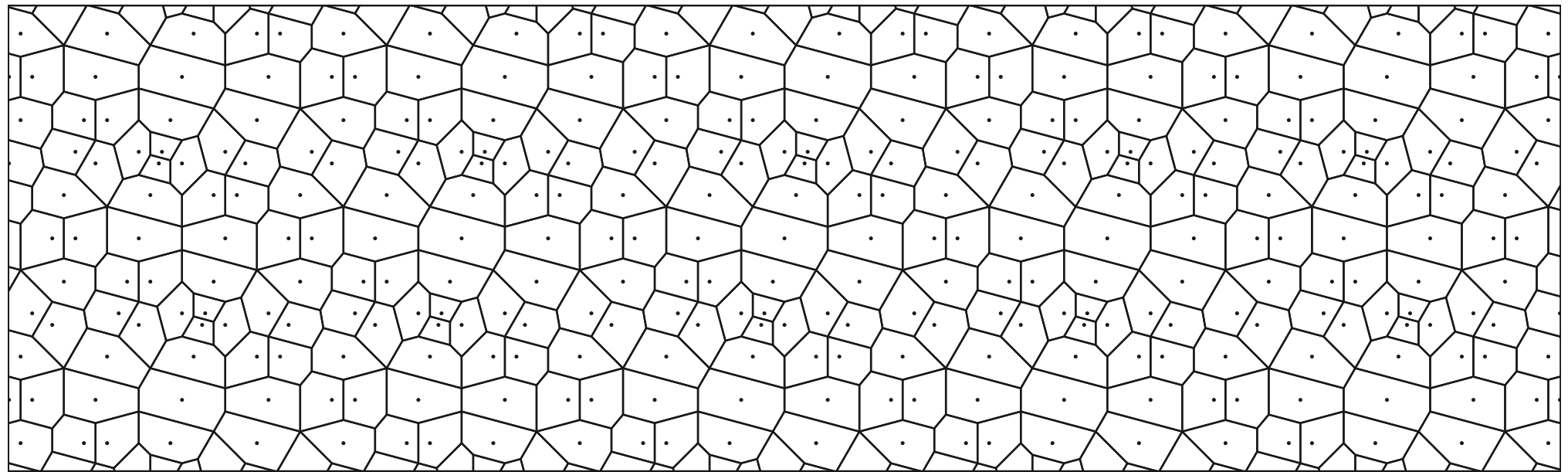
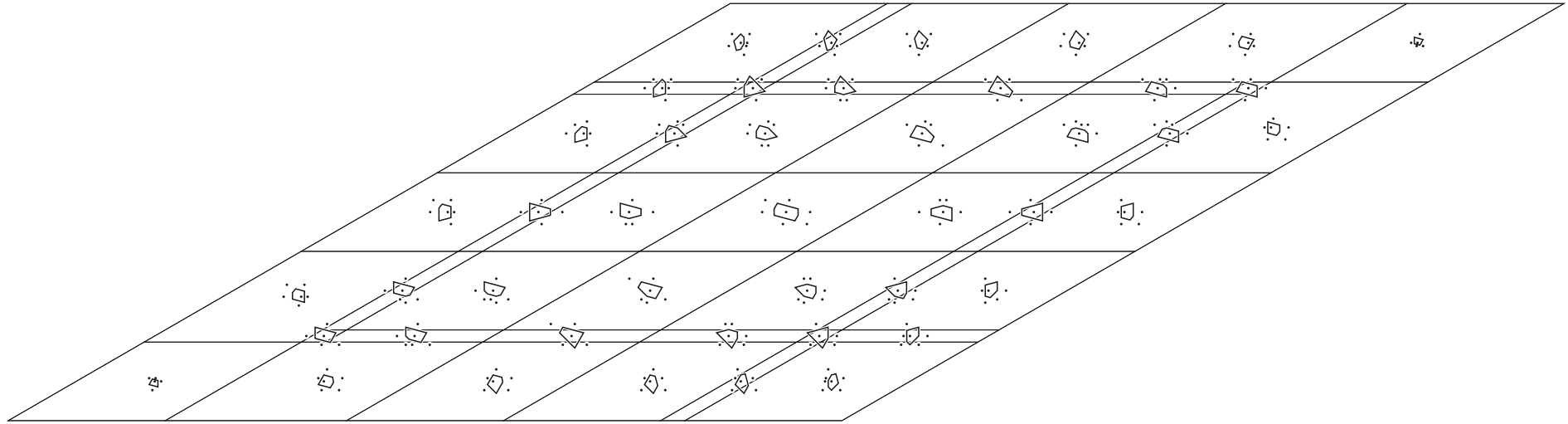


$4 - \beta$

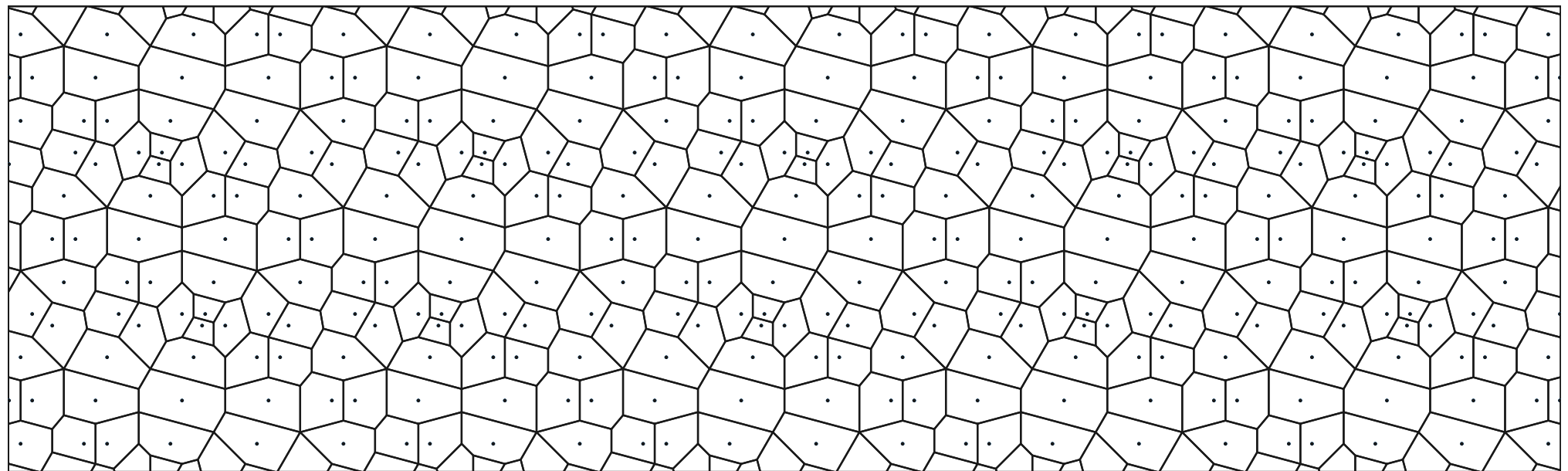
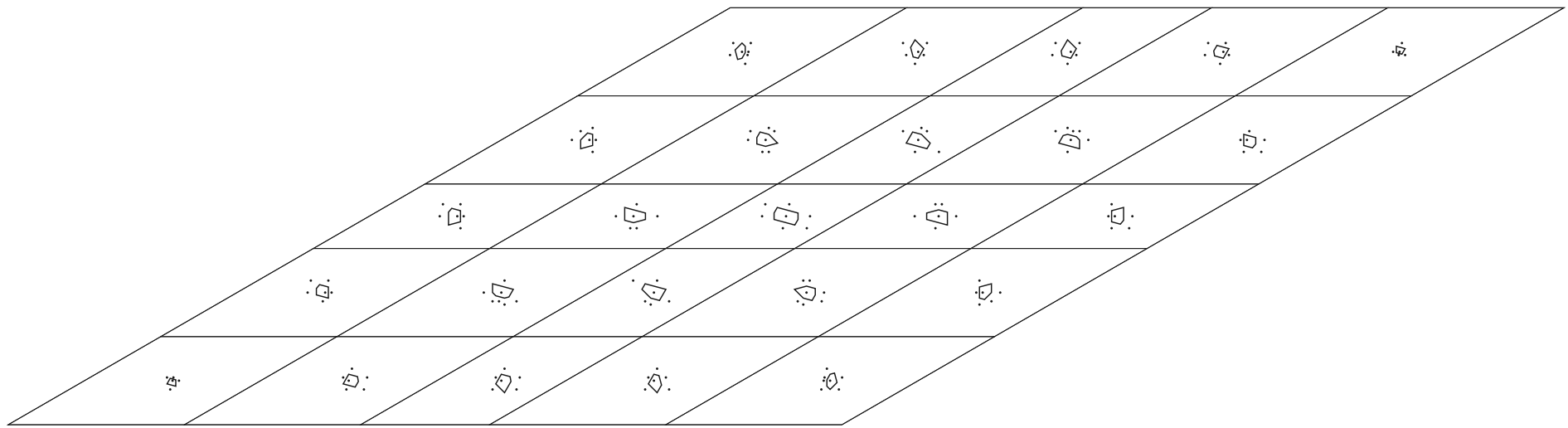


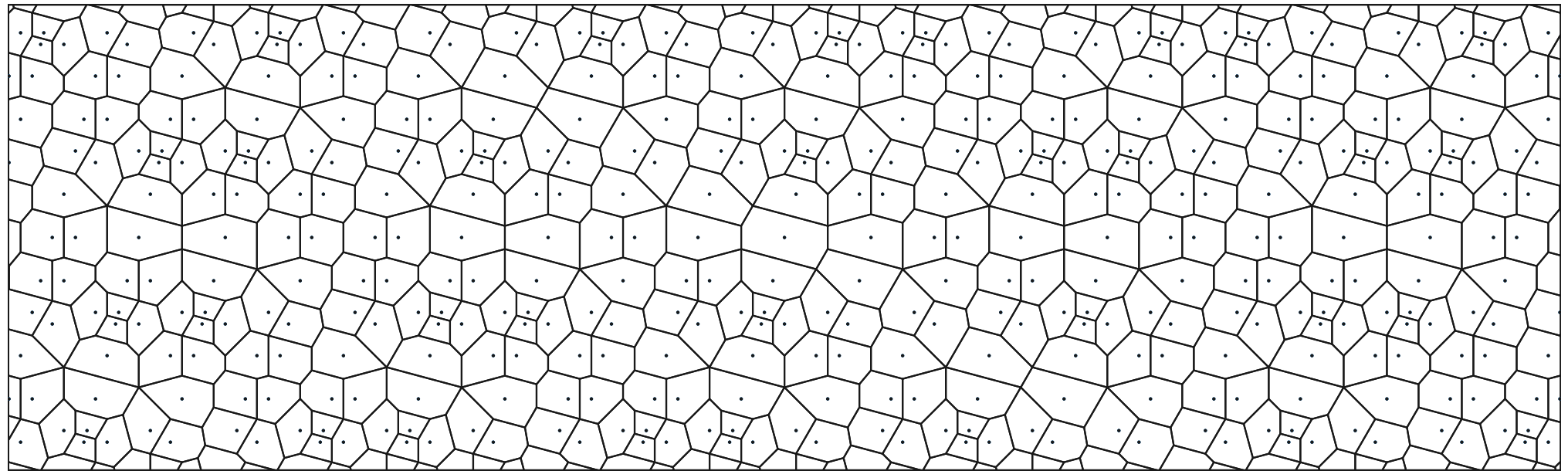
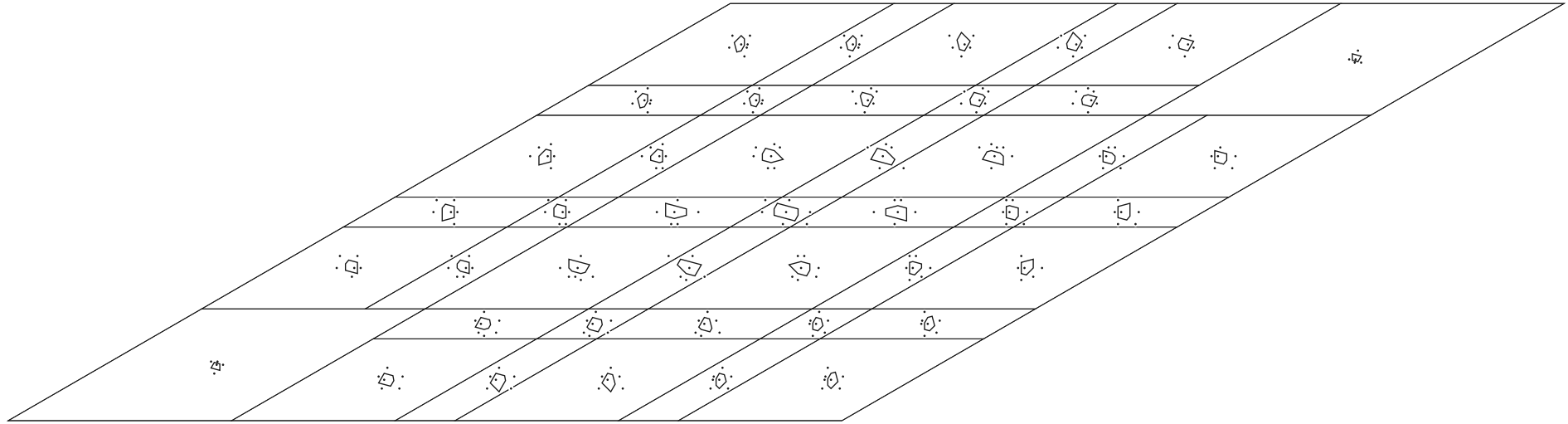
$$\frac{9\beta - 33}{2}$$



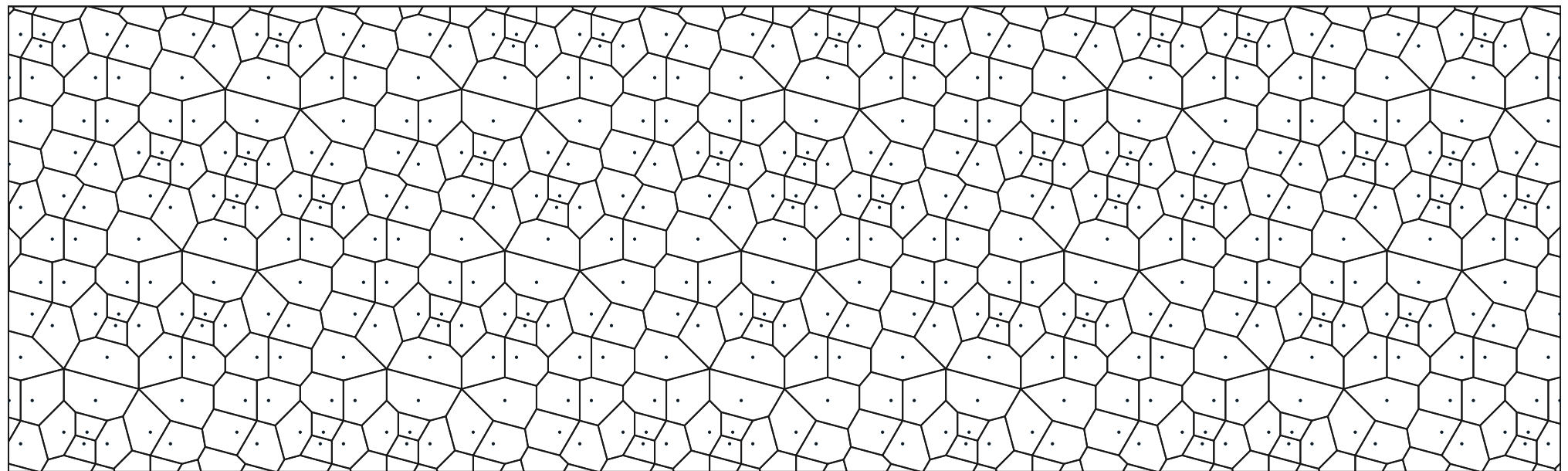
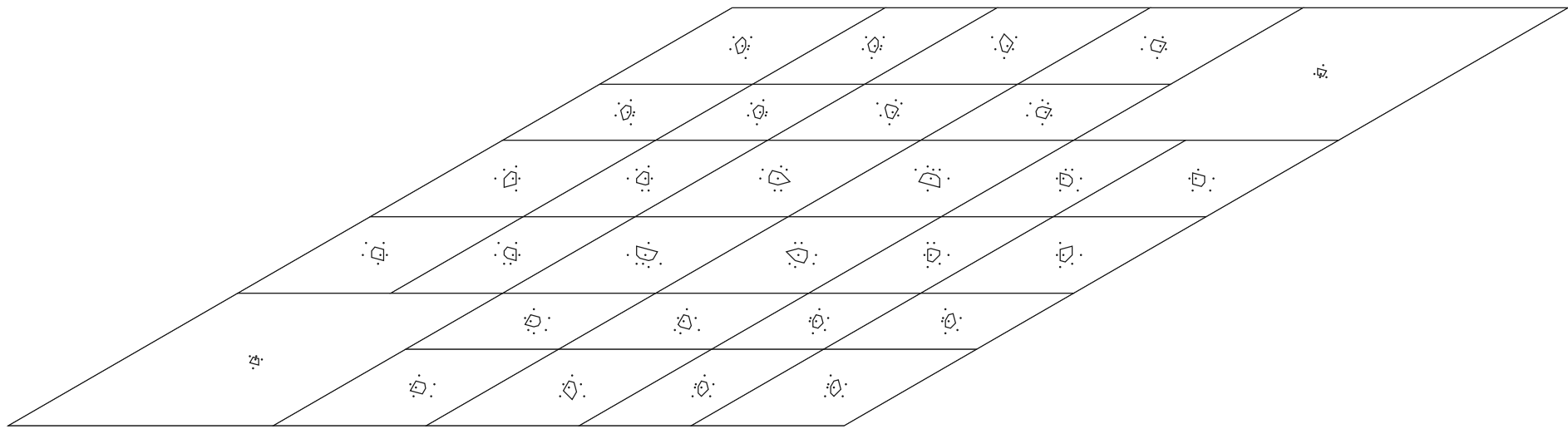


$$\frac{5\beta - 18}{2}$$

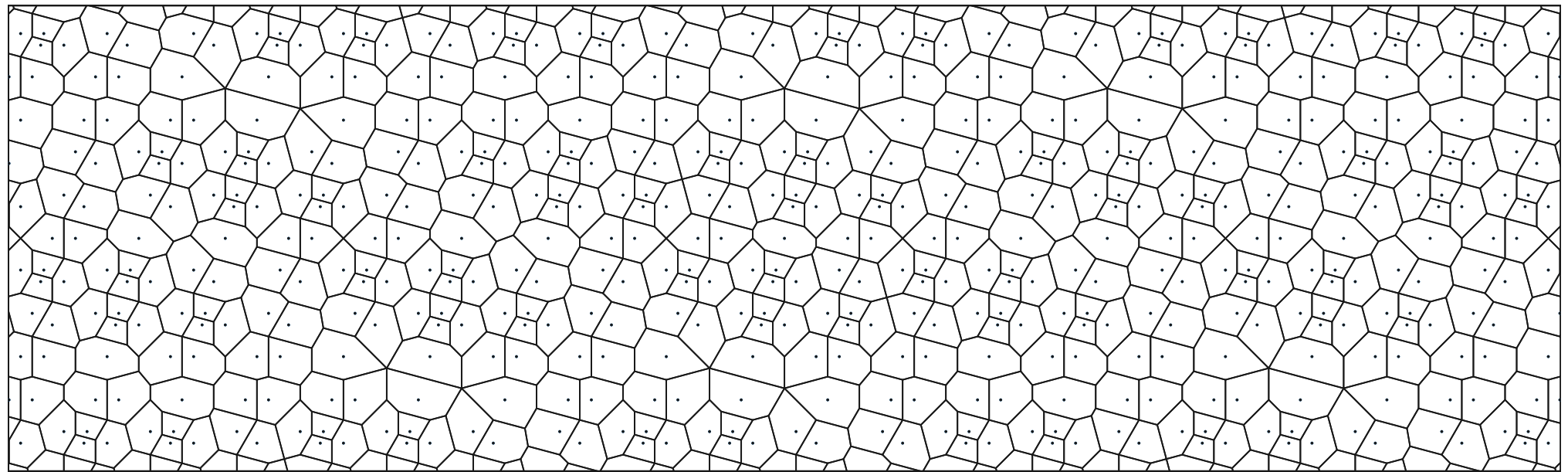
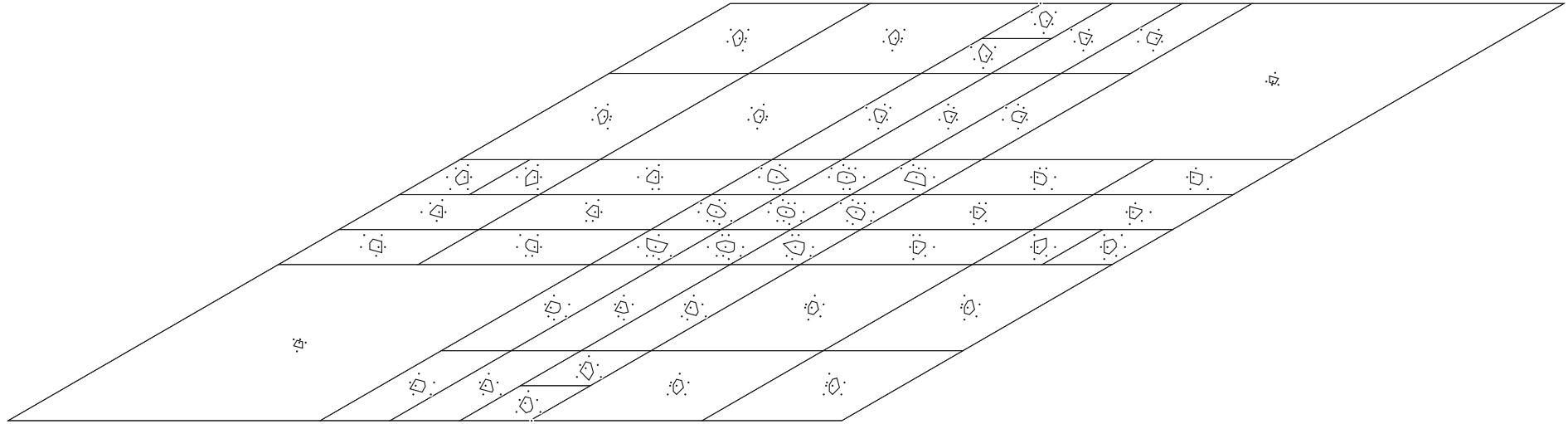




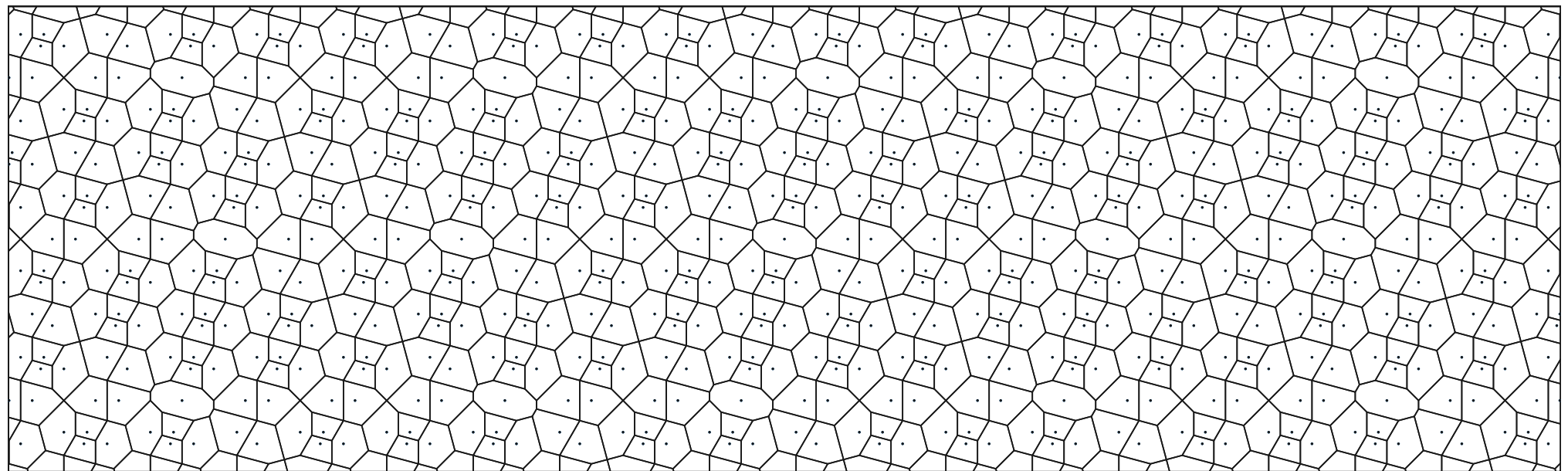
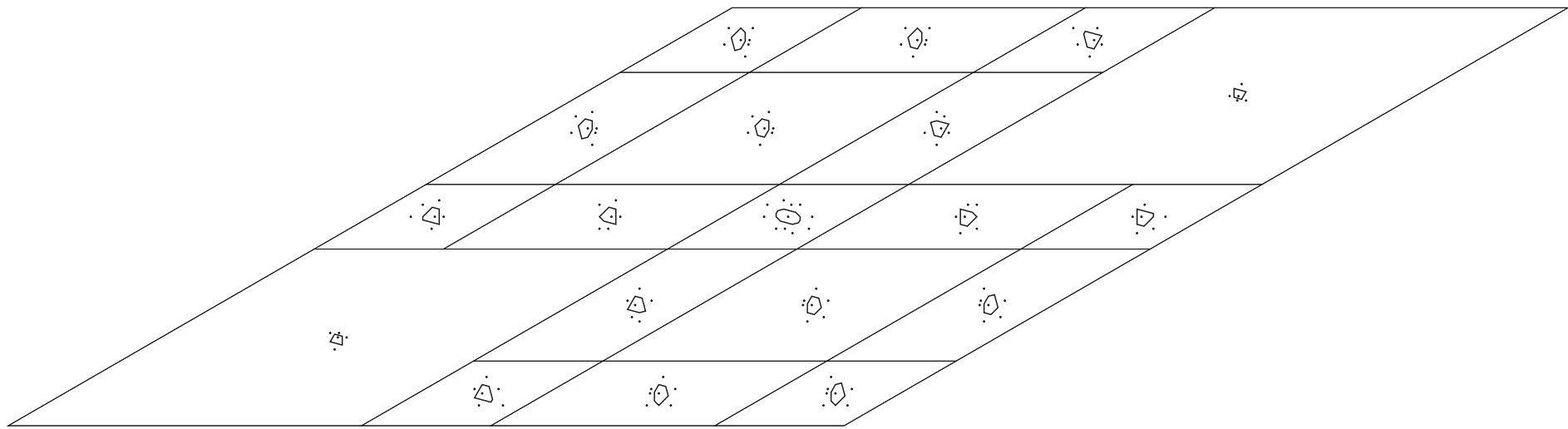
$$\frac{\beta-3}{2}$$



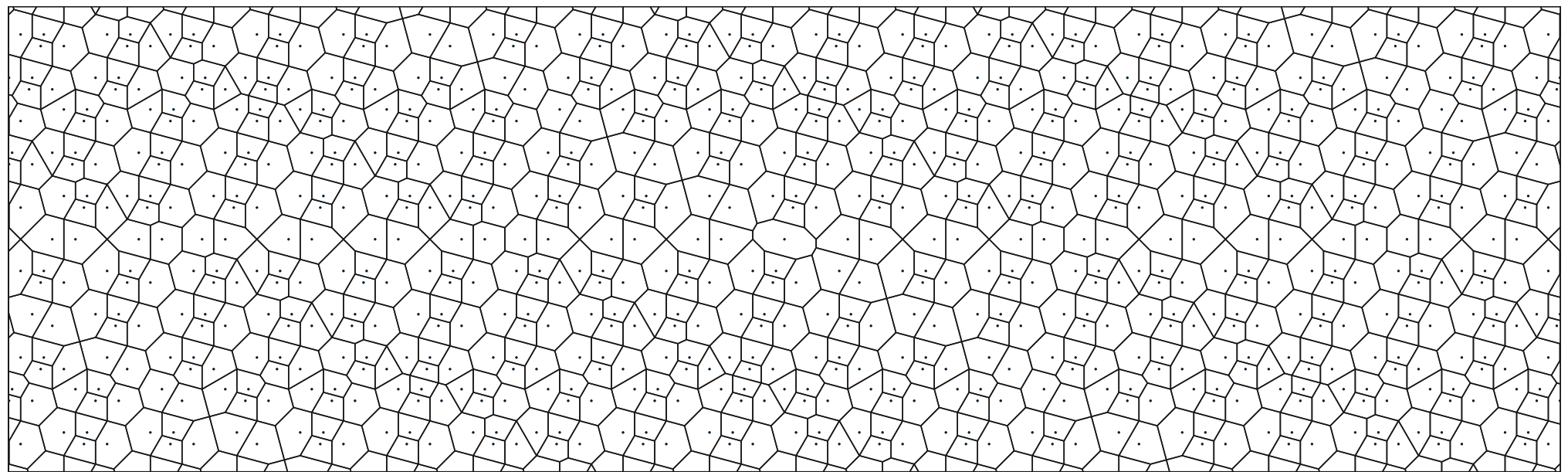
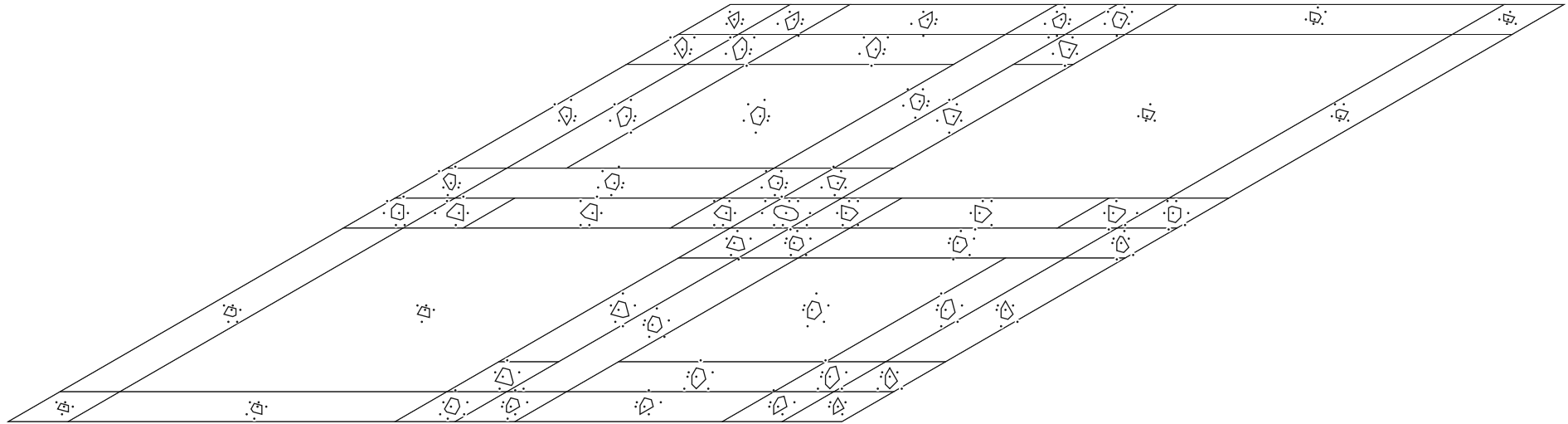
$6\beta - 22$

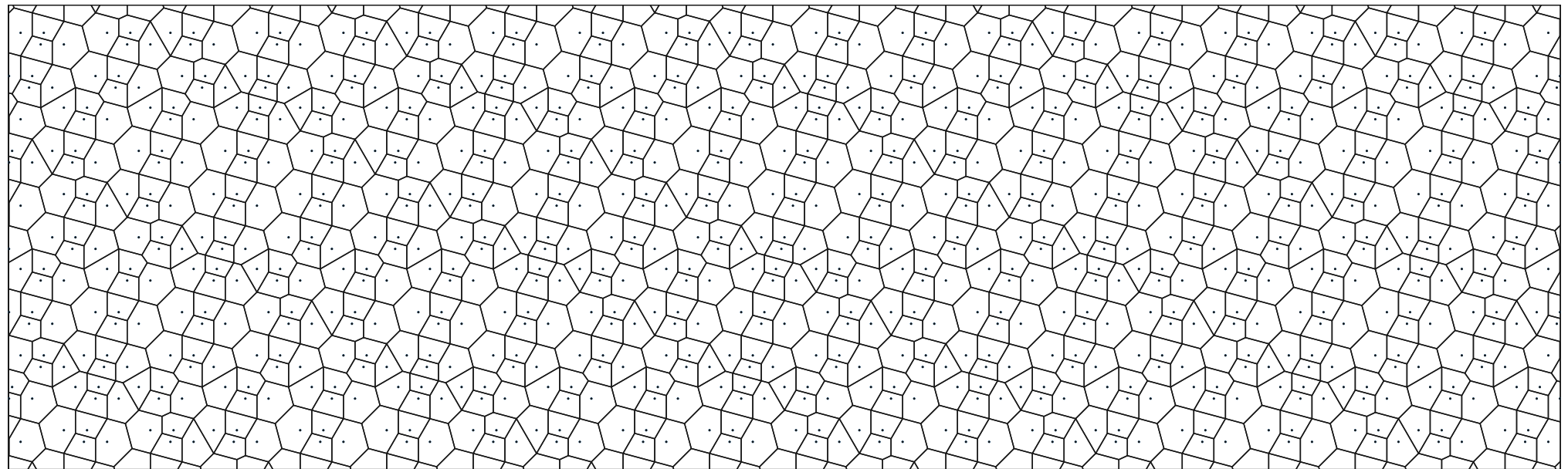
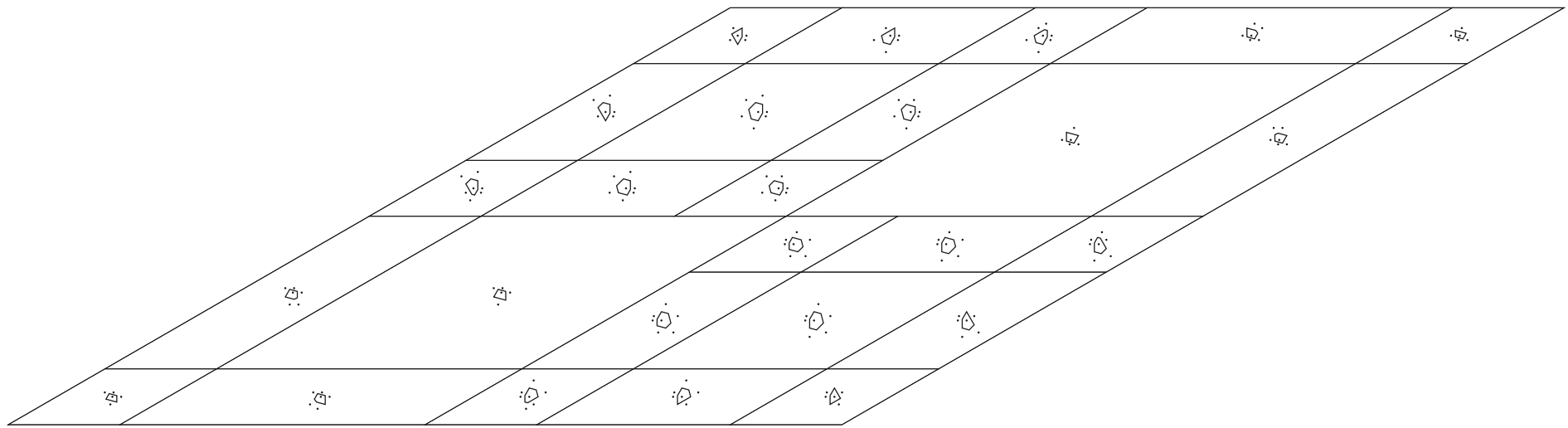


$$\frac{8\beta - 29}{2}$$

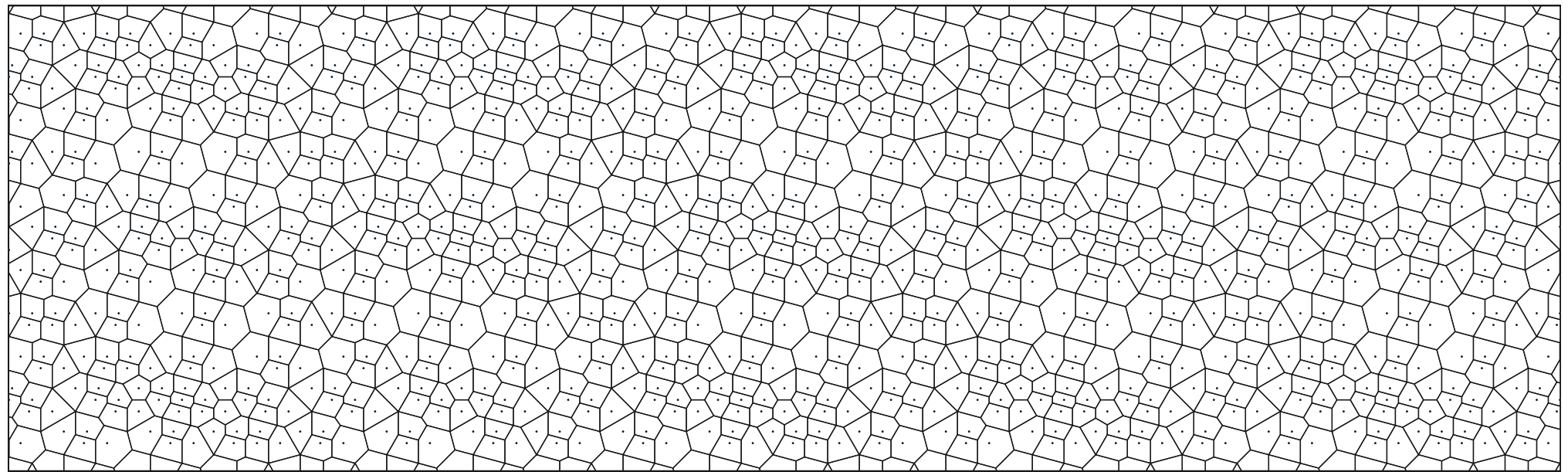
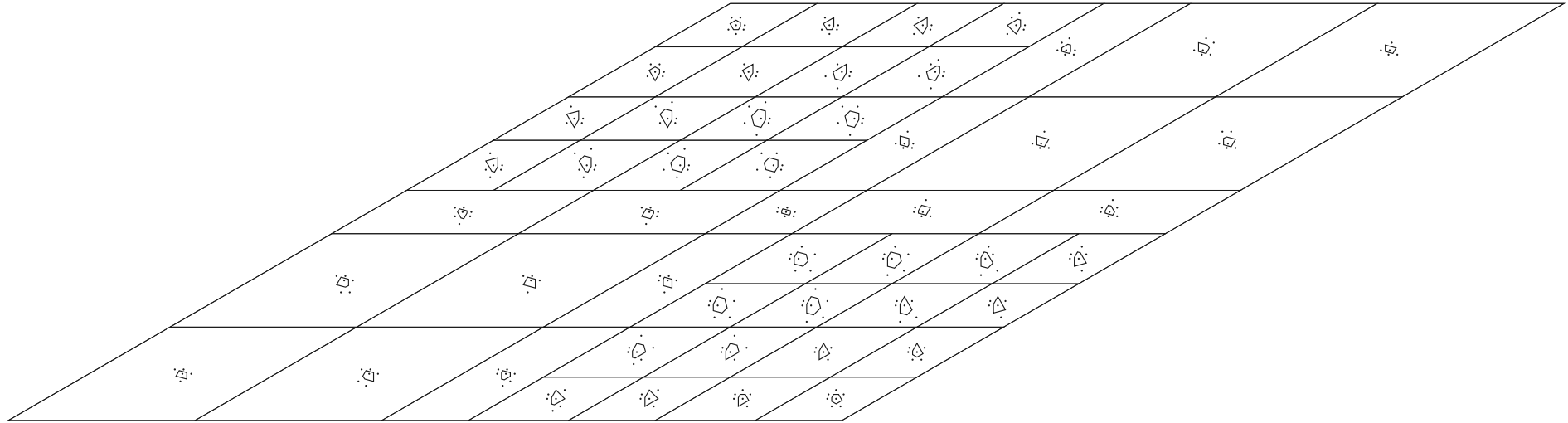


$$2\beta - 7$$

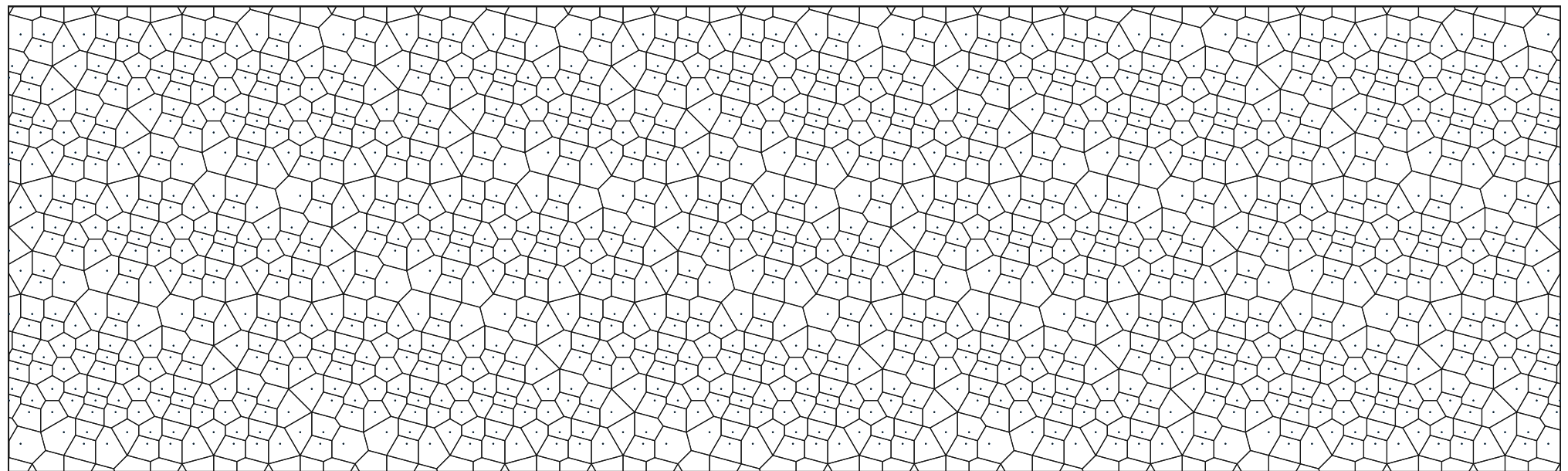
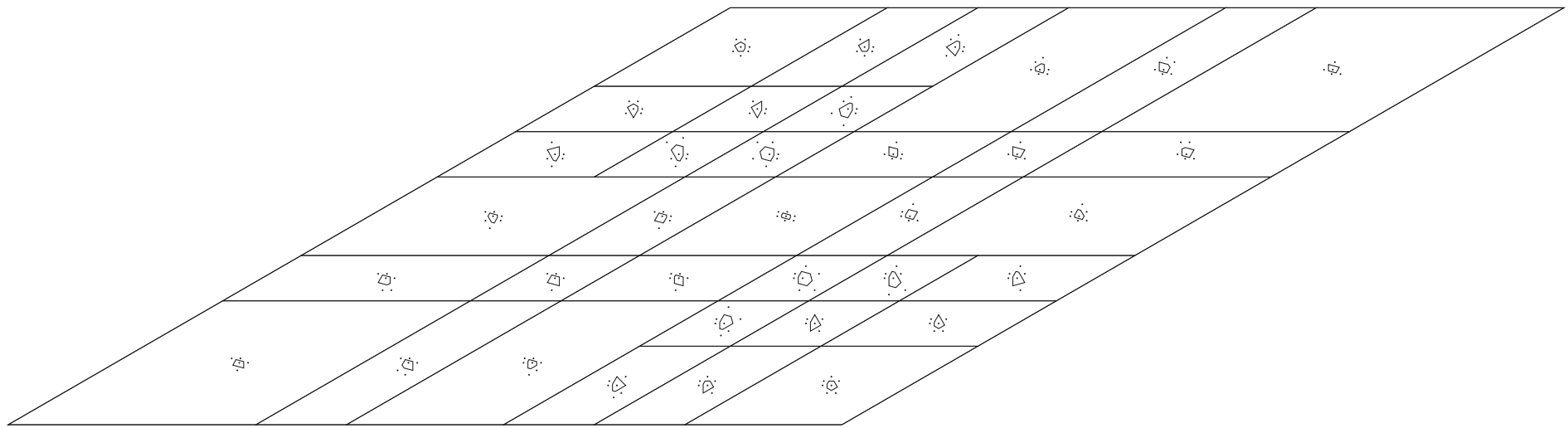




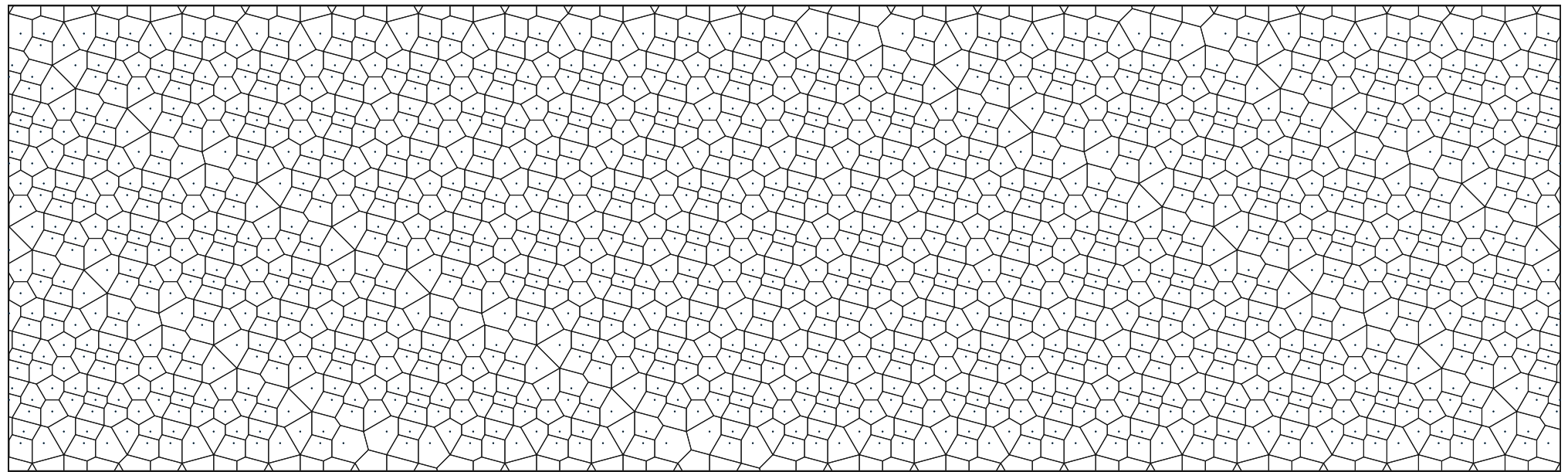
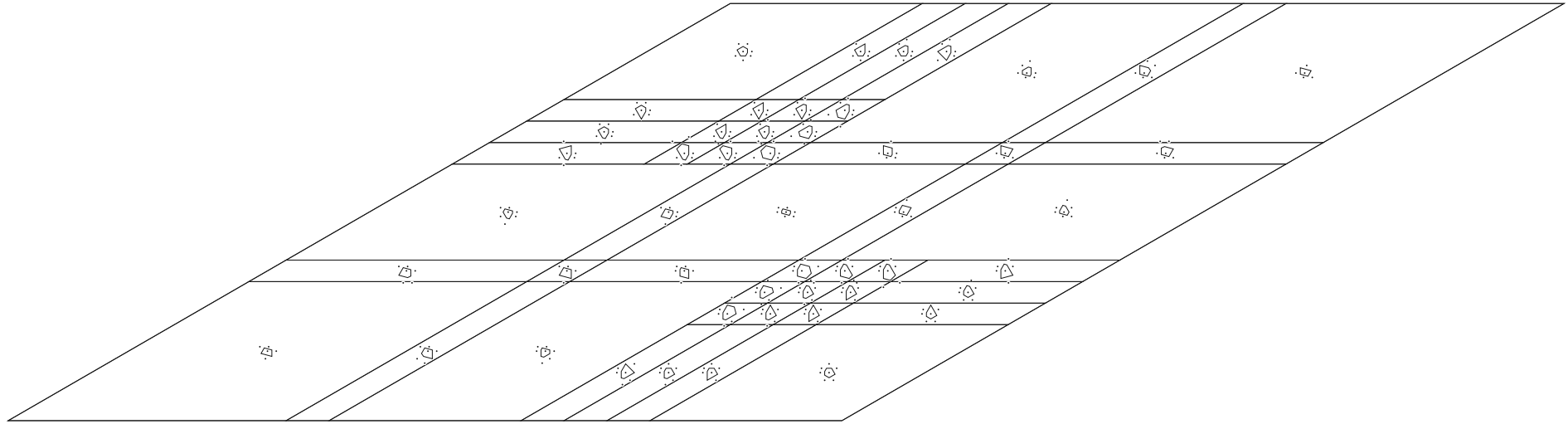
$$8 - 2\beta$$



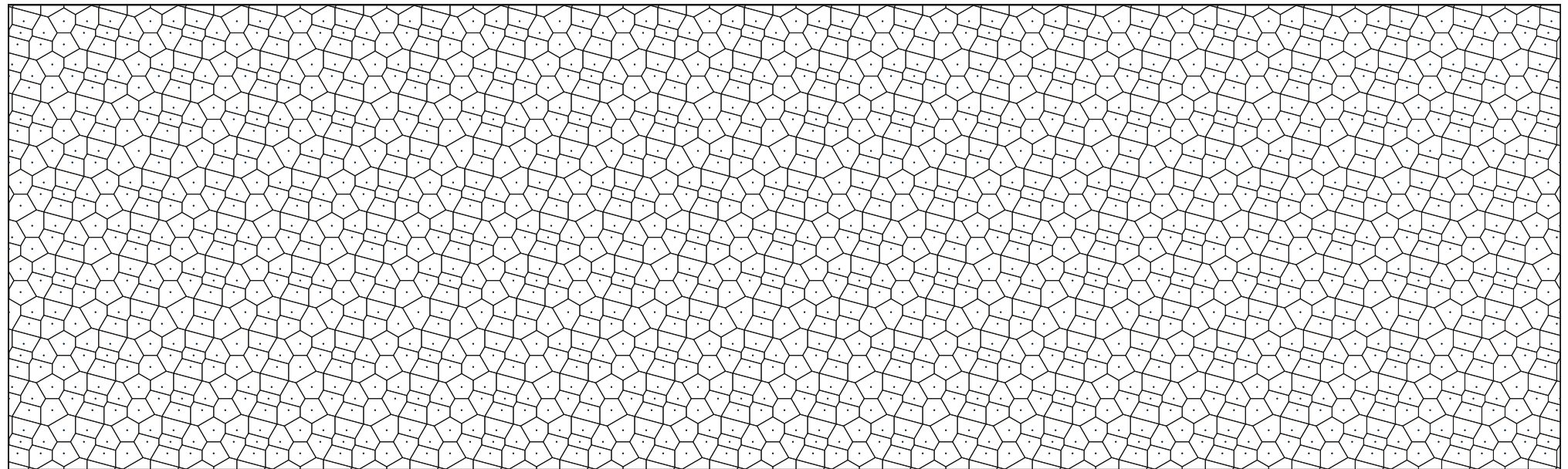
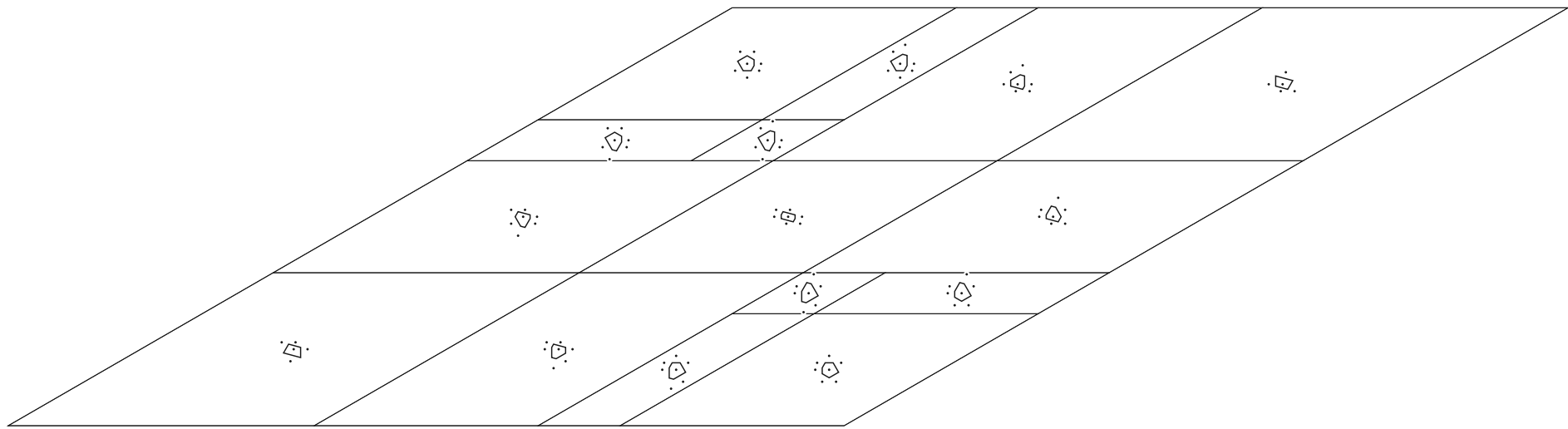
$$\frac{3\beta - 10}{2}$$



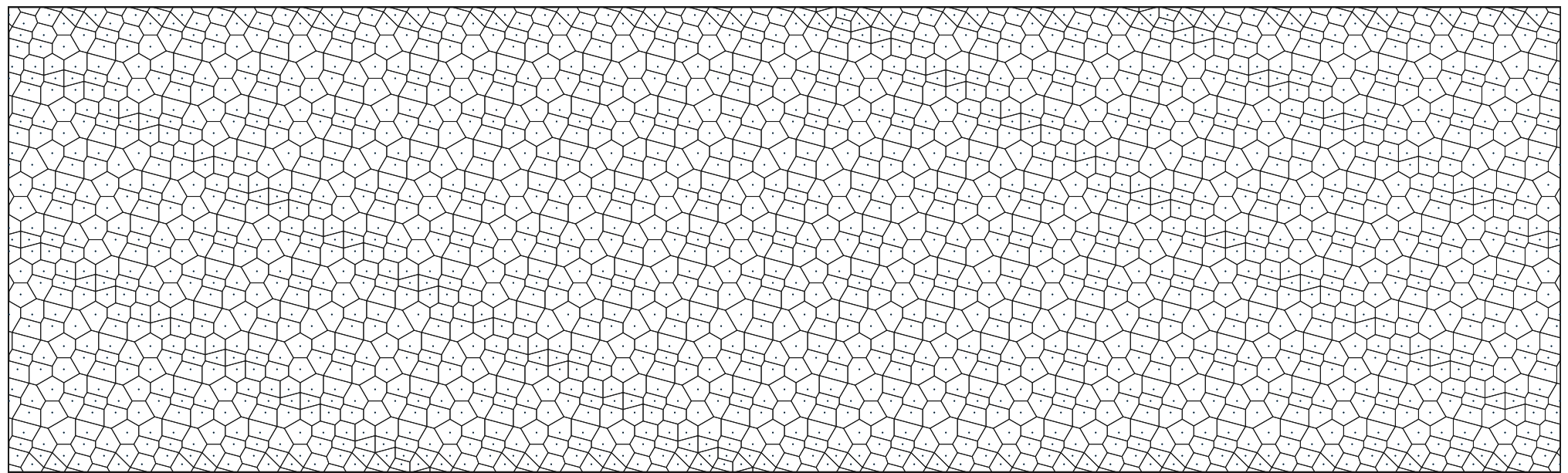
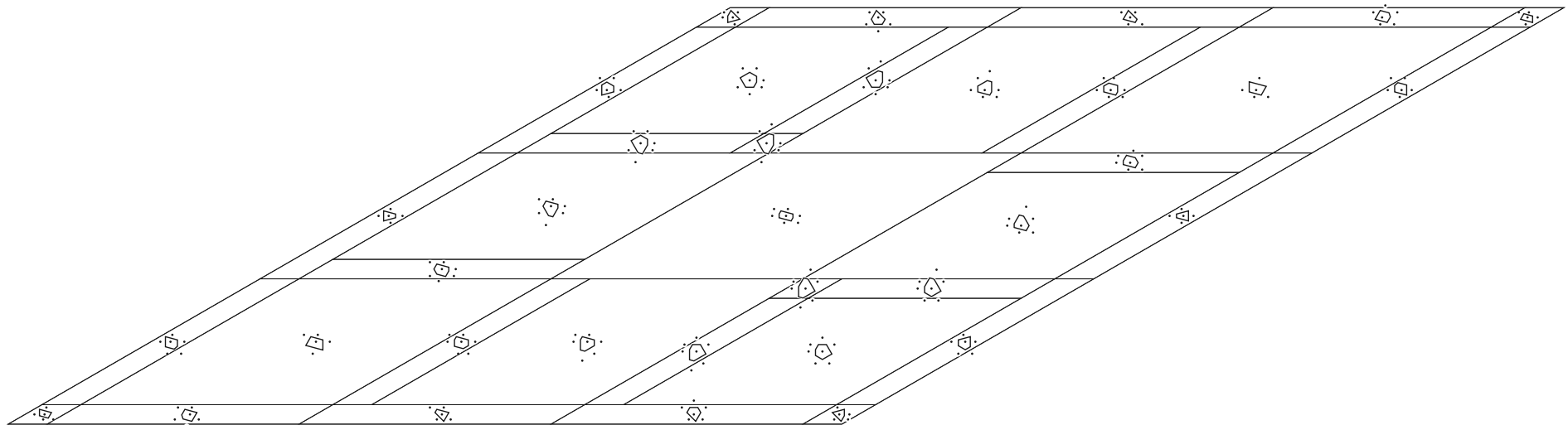
$5\beta - 18$



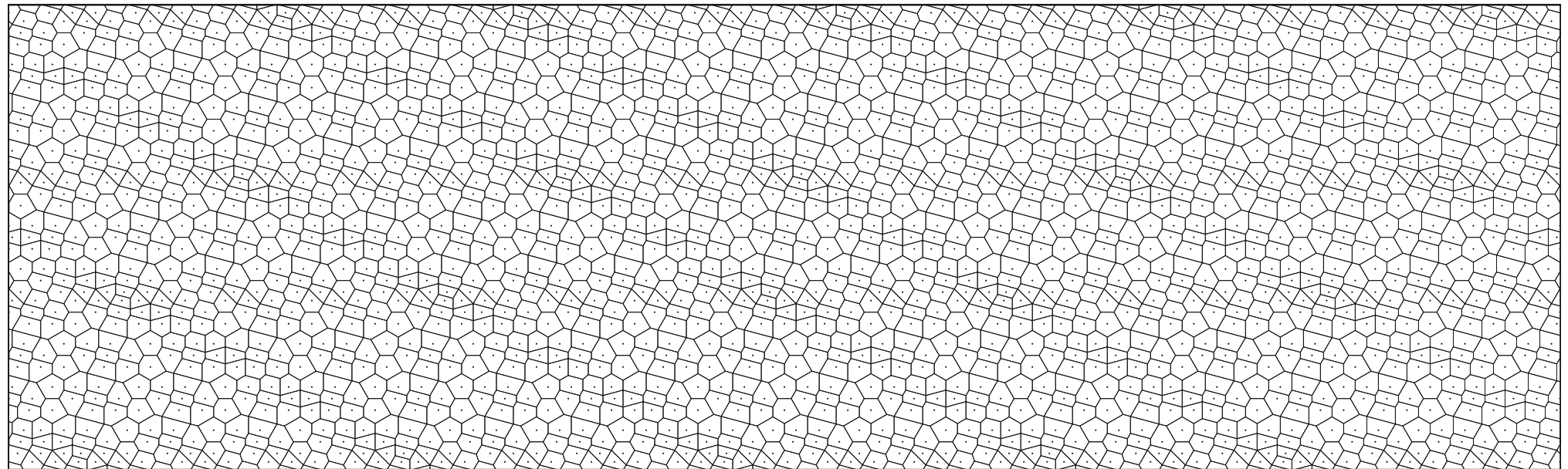
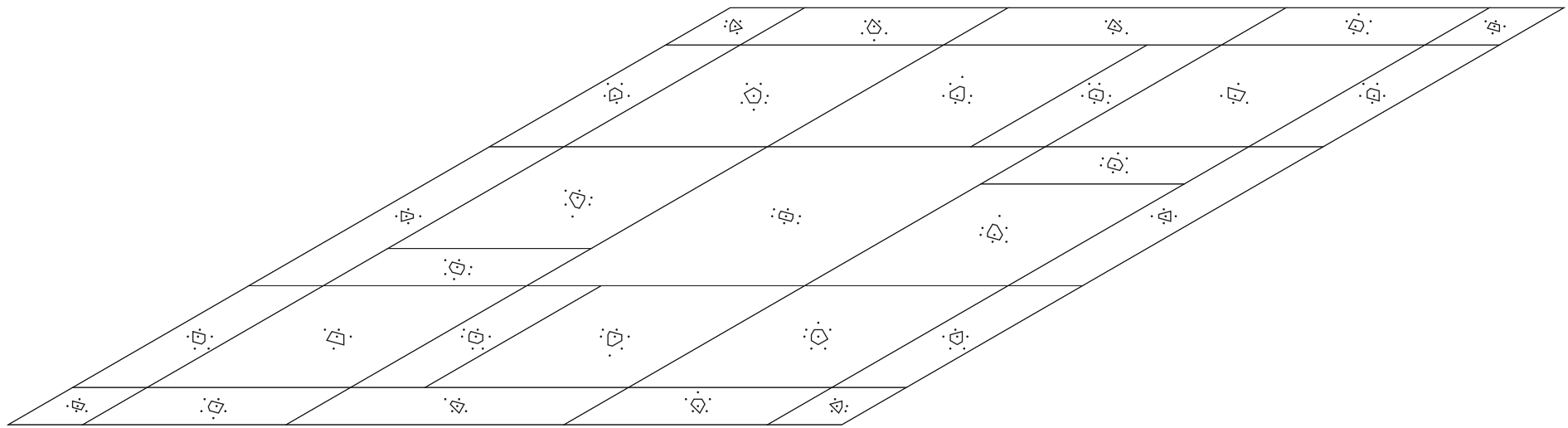
$$\frac{6\beta - 21}{2}$$



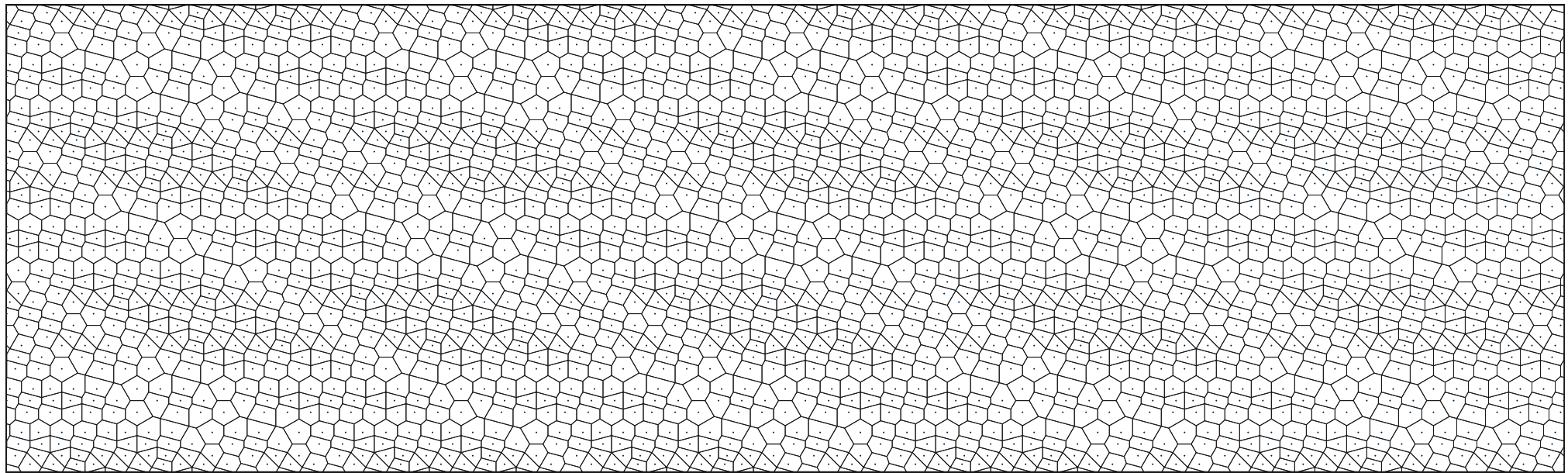
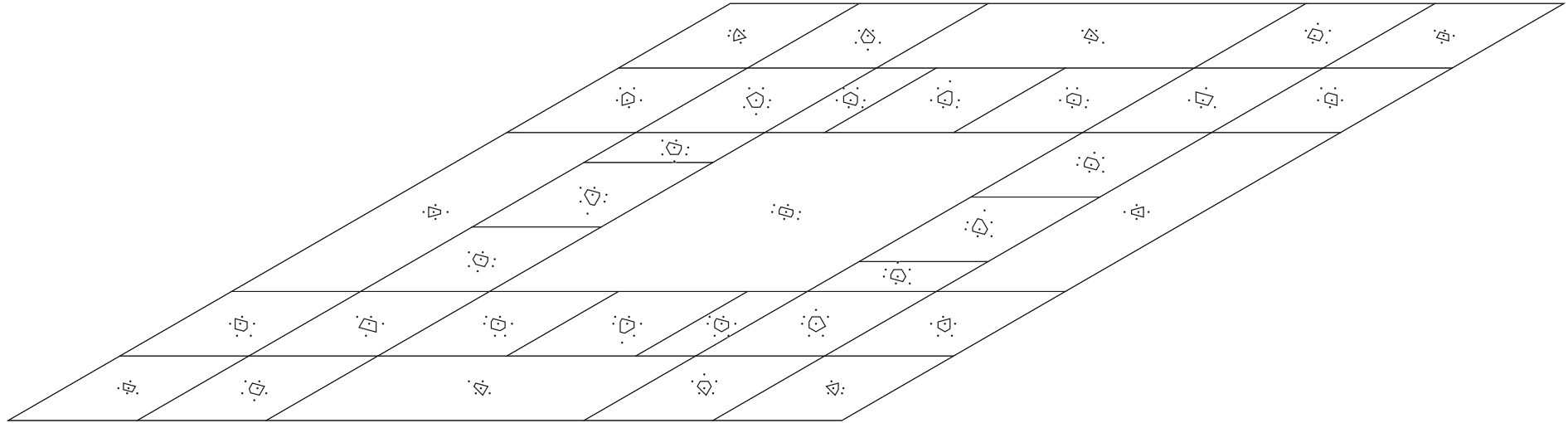
$\beta - 3$



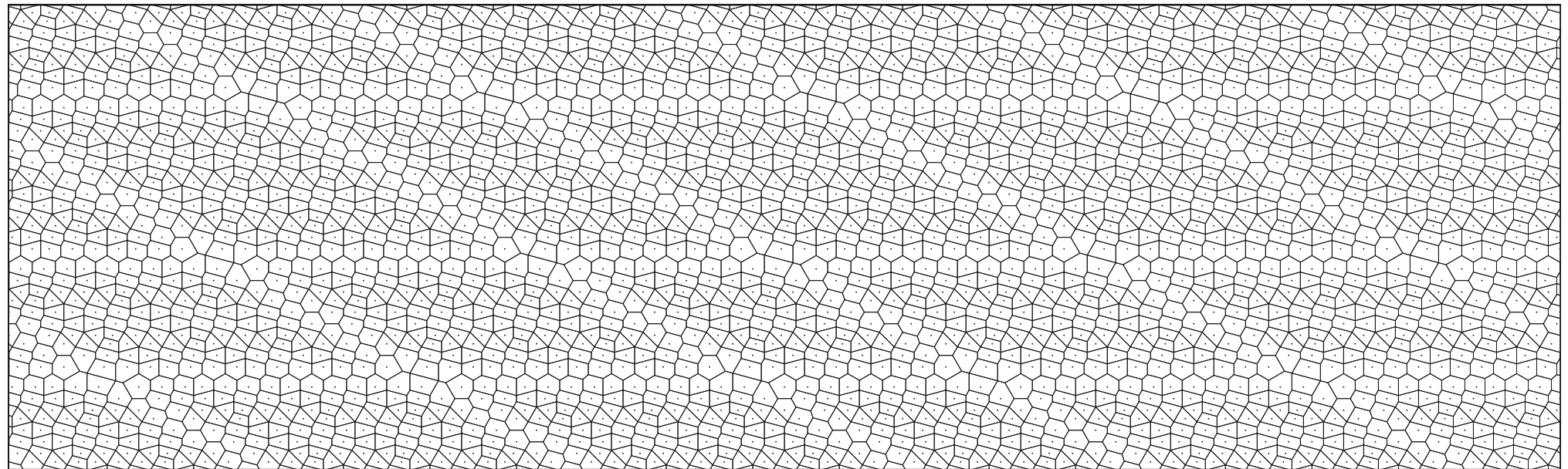
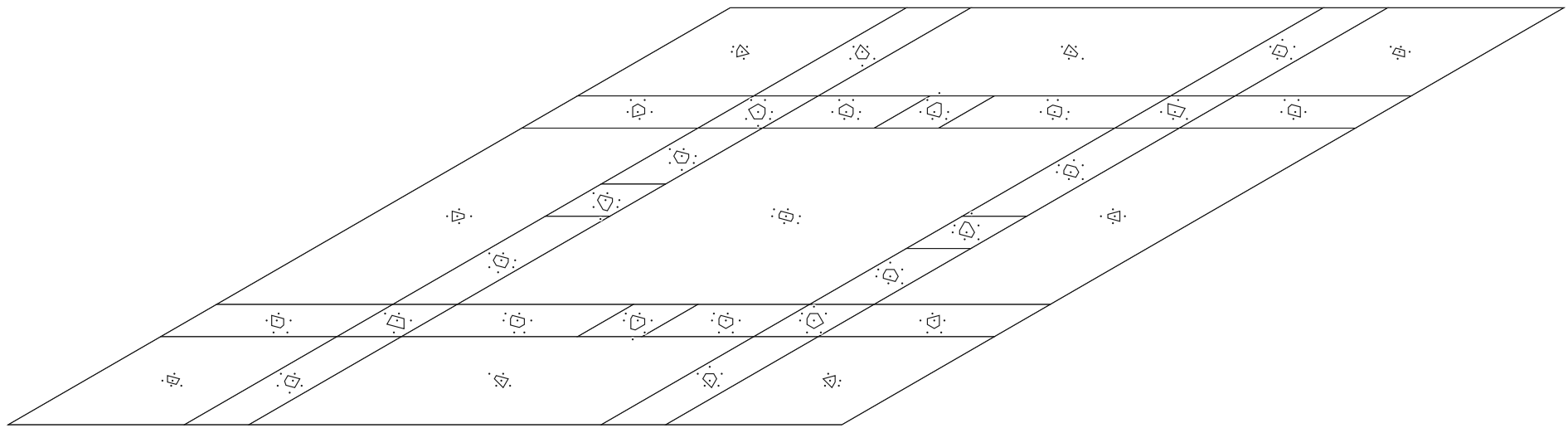
$$\frac{9-2\beta}{2}$$



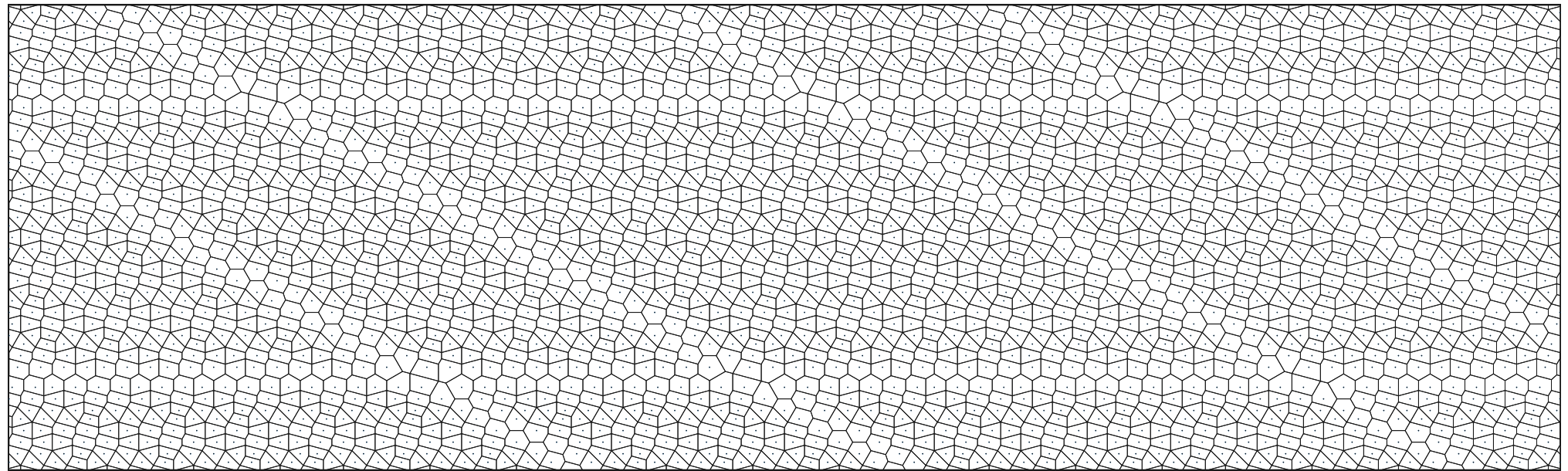
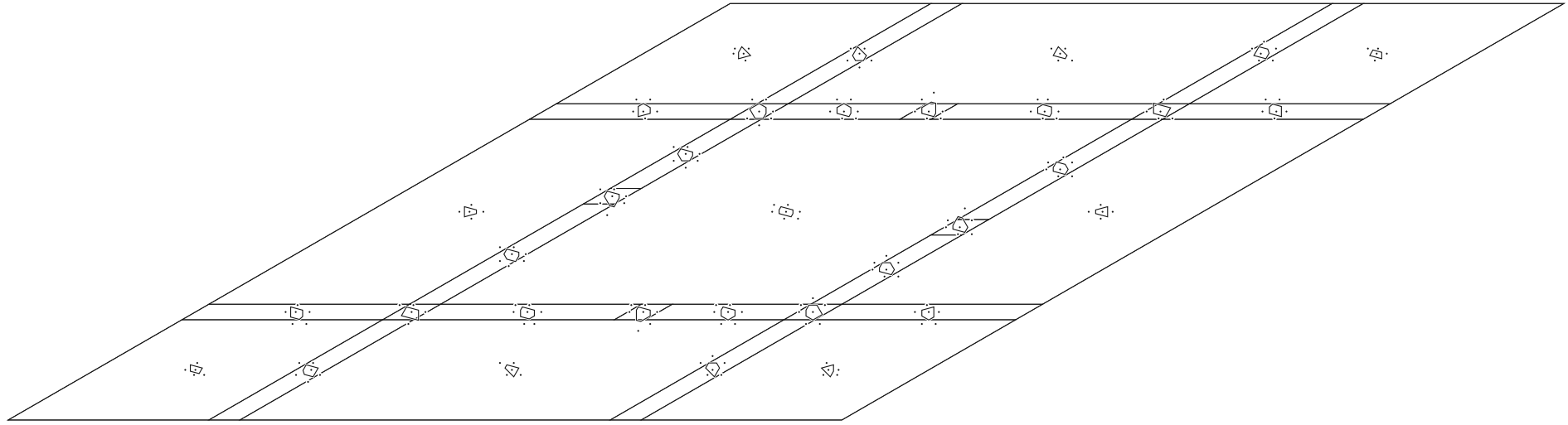
$12 - 3\beta$



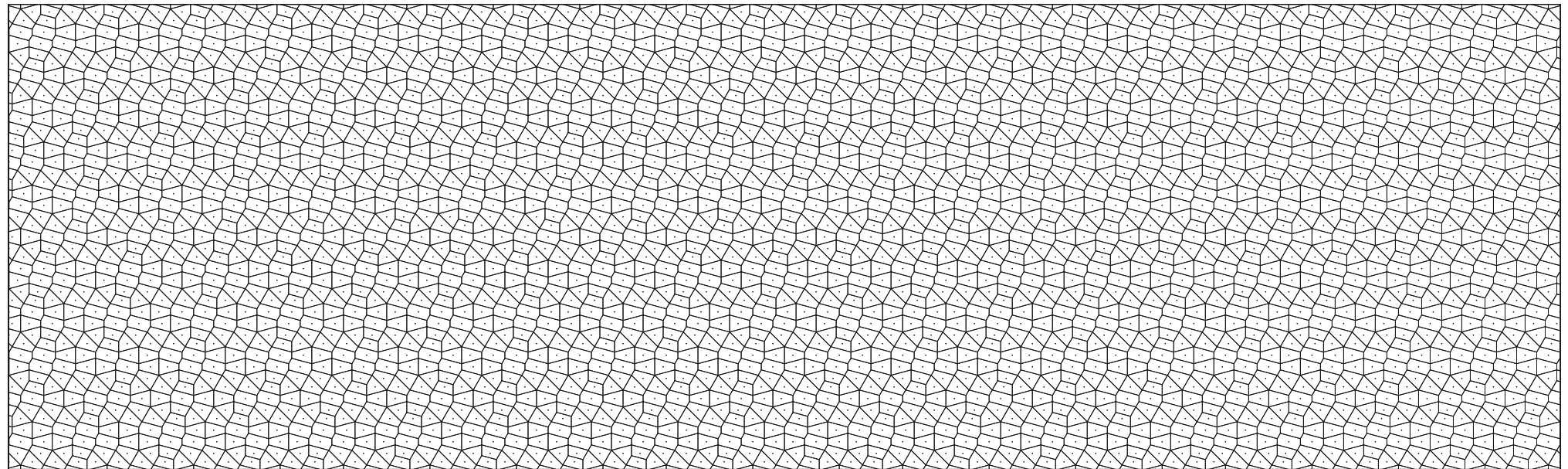
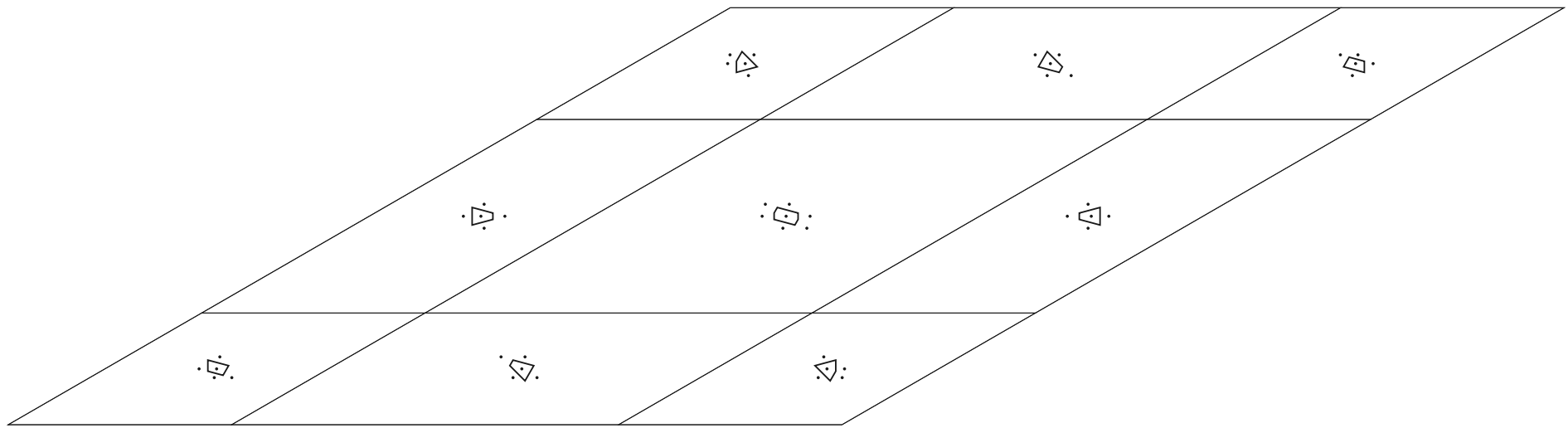
$$\frac{\beta-2}{2}$$



$4\beta - 14$



$$\frac{4\beta - 13}{2}$$



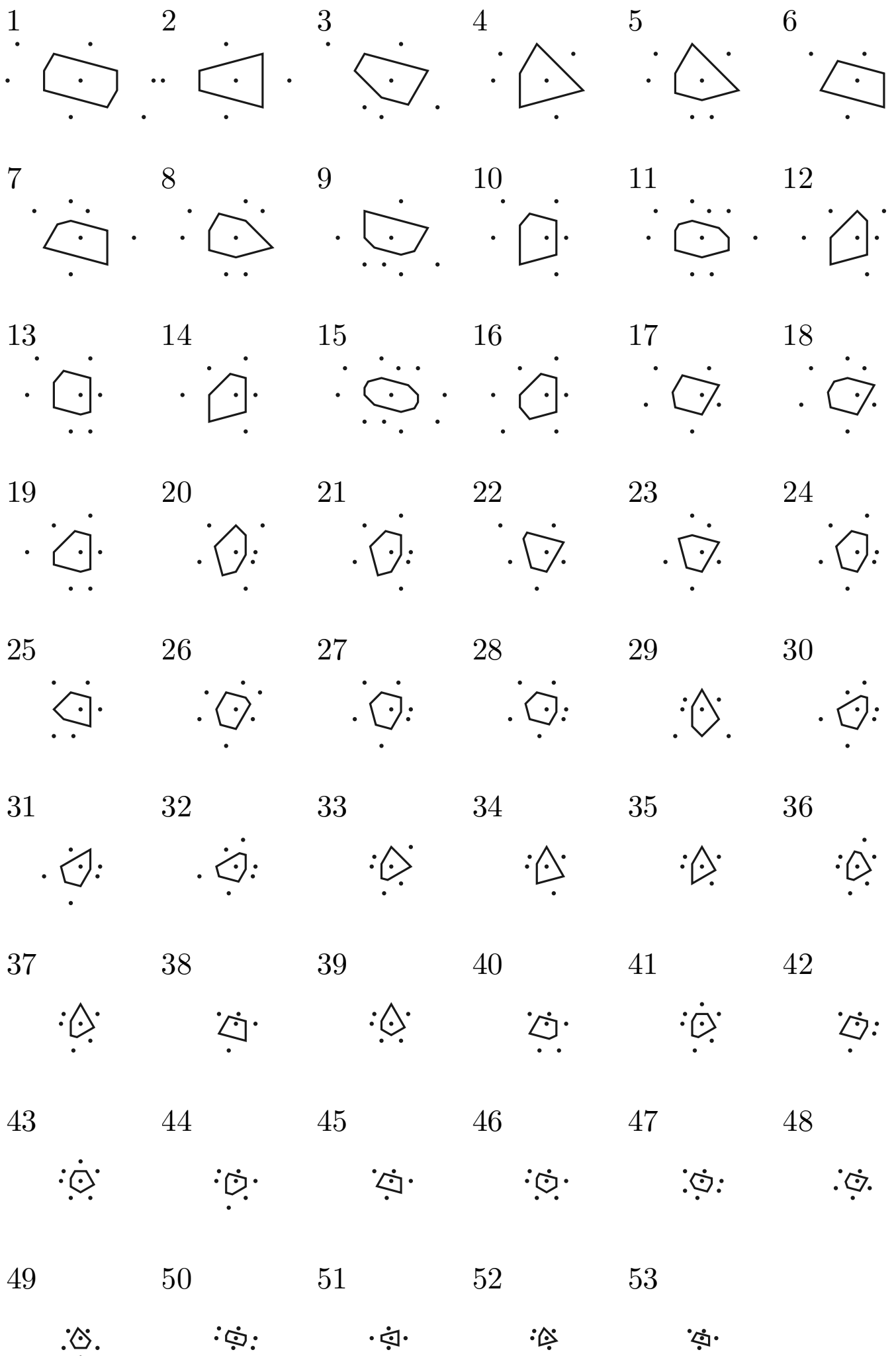


Table 2: Assignment of voronoi polygons to their quasicrystals. Horizontal axis enumerates members of  $\mathcal{D}$  and the vertical axis corresponds to the numbers from the list of voronoi polygons.

|    | 1 | 2 | 3 | 4 | 5 | 6 | 7 | 8 | 9 | 10 | 11 | 12 | 13 | 14 | 15 | 16 | 17 | 18 | 19 | 20 | 21 |
|----|---|---|---|---|---|---|---|---|---|----|----|----|----|----|----|----|----|----|----|----|----|
| 1  | • | • | • | • |   |   |   |   |   |    |    |    |    |    |    |    |    |    |    |    |    |
| 2  | • | • | • | • | • | • | • | • | • | •  |    |    |    |    |    |    |    |    |    |    |    |
| 3  |   | • | • | • |   |   |   |   |   |    |    |    |    |    |    |    |    |    |    |    |    |
| 4  | • | • | • | • |   |   |   |   |   |    |    |    |    |    |    |    |    |    |    |    |    |
| 5  |   | • | • | • |   |   |   |   |   |    |    |    |    |    |    |    |    |    |    |    |    |
| 6  | • | • | • | • | • | • | • | • | • | •  |    |    |    |    |    |    |    |    |    |    |    |
| 7  |   | • | • | • | • | • | • |   |   |    |    |    |    |    |    |    |    |    |    |    |    |
| 8  | • | • | • | • |   |   |   |   |   |    |    |    |    |    |    |    |    |    |    |    |    |
| 9  |   | • | • | • | • | • | • | • | • | •  | •  |    |    |    |    |    |    |    |    |    |    |
| 10 | • | • | • | • | • | • | • | • | • | •  | •  |    |    |    |    |    |    |    |    |    |    |
| 11 |   |   |   |   |   |   | • |   |   |    |    |    |    |    |    |    |    |    |    |    |    |
| 12 | • | • | • | • | • | • | • | • | • | •  | •  | •  | •  | •  | •  | •  | •  | •  | •  | •  | •  |
| 13 |   |   |   |   |   | • |   |   |   |    |    |    |    |    |    |    |    |    |    |    |    |
| 14 | • | • | • | • |   |   |   |   |   |    |    |    |    |    |    |    |    |    |    |    |    |
| 15 |   |   |   |   | • | • | • |   |   |    |    |    |    |    |    |    |    |    |    |    |    |
| 16 |   |   |   |   |   | • |   |   |   |    |    |    |    |    |    |    |    |    |    |    |    |
| 17 | • | • | • | • | • | • | • | • | • | •  |    |    |    |    |    |    |    |    |    |    |    |
| 18 |   |   |   |   | • | • | • |   |   |    |    |    |    |    |    |    |    |    |    |    |    |
| 19 |   |   |   |   |   |   |   | • | • | •  | •  | •  | •  | •  | •  | •  | •  | •  | •  | •  | •  |
| 20 | • | • | • | • | • | • |   |   |   |    |    |    |    |    |    |    |    |    |    |    |    |
| 21 |   |   |   | • | • | • | • | • | • | •  | •  | •  | •  | •  | •  | •  | •  | •  | •  | •  | •  |
| 22 |   |   |   |   | • | • | • | • | • | •  | •  | •  | •  | •  | •  | •  | •  | •  | •  | •  | •  |
| 23 |   |   |   |   |   | • | • | • | • | •  | •  | •  | •  | •  | •  | •  | •  | •  | •  | •  | •  |
| 24 |   |   |   |   | • | • | • | • | • | •  | •  | •  | •  | •  | •  | •  | •  | •  | •  | •  | •  |
| 25 |   |   |   |   |   |   | • |   |   |    |    |    |    |    |    |    |    |    |    |    |    |
| 26 |   |   |   |   |   |   |   | • |   |    |    |    |    |    |    |    |    |    |    |    |    |
| 27 |   |   |   |   |   |   |   |   | • |    |    |    |    |    |    |    |    |    |    |    |    |
| 28 |   |   |   |   |   |   |   |   |   | •  |    |    |    |    |    |    |    |    |    |    |    |
| 29 |   |   |   |   |   |   |   |   |   | •  |    |    |    |    |    |    |    |    |    |    |    |
| 30 |   |   |   |   |   |   |   |   |   |    | •  |    |    |    |    |    |    |    |    |    |    |
| 31 |   |   |   |   |   |   |   |   |   |    | •  |    |    |    |    |    |    |    |    |    |    |
| 32 |   |   |   |   |   |   |   |   |   |    |    | •  |    |    |    |    |    |    |    |    |    |
| 33 |   |   |   |   |   |   |   |   |   |    |    | •  |    |    |    |    |    |    |    |    |    |
| 34 |   |   |   |   |   |   |   |   |   |    |    |    | •  |    |    |    |    |    |    |    |    |
| 35 |   |   |   |   |   |   |   |   |   | •  |    | •  |    |    |    |    |    |    |    |    |    |
| 36 |   |   |   |   |   |   |   |   |   |    |    |    | •  |    |    |    |    |    |    |    |    |
| 37 |   |   |   |   |   |   |   |   |   |    |    |    |    | •  |    |    |    |    |    |    |    |
| 38 | • | • | • | • | • | • |   |   |   |    |    |    |    |    |    |    |    |    |    |    |    |
| 39 |   |   |   |   |   |   |   |   |   |    |    |    |    | •  | •  | •  | •  | •  | •  | •  | •  |
| 40 |   |   |   |   |   |   |   |   |   | •  |    | •  |    | •  | •  | •  | •  | •  | •  | •  | •  |
| 41 |   |   |   |   |   |   |   |   |   |    |    |    |    | •  |    |    |    |    |    |    |    |
| 42 |   |   |   |   |   |   |   |   |   |    |    |    |    |    | •  |    |    |    |    |    |    |
| 43 |   |   |   |   |   |   |   |   |   |    |    |    |    |    |    | •  |    |    |    |    |    |
| 44 |   |   |   |   | • | • | • | • |   |    |    |    |    |    |    |    |    |    |    |    |    |
| 45 |   |   |   |   |   |   |   |   | • |    |    |    |    |    |    |    |    |    |    |    |    |
| 46 |   |   |   |   |   |   |   |   |   |    |    |    |    |    |    |    | •  |    |    |    |    |
| 47 |   |   |   |   |   |   |   |   |   |    |    |    |    |    |    |    |    | •  |    |    |    |
| 48 |   |   |   |   |   |   |   |   |   |    |    |    |    |    |    |    |    | •  |    |    |    |
| 49 |   |   |   |   |   |   |   |   |   |    |    |    |    |    |    |    |    | •  |    |    |    |
| 50 |   |   |   |   |   |   |   |   |   |    |    |    |    |    |    |    |    | •  |    |    |    |
| 51 |   |   |   |   |   |   |   |   |   |    |    |    |    |    |    |    |    | •  |    |    |    |
| 52 |   |   |   |   |   |   |   |   |   |    |    |    |    |    |    |    |    | •  |    |    |    |
| 53 |   |   |   |   |   |   |   |   |   |    |    |    |    |    |    |    |    | •  |    |    |    |

